

## **Final Scientific Report**

**Project Title:**        **Characterization of Fine Particulate Matter (PM) and  
Secondary PM Precursor Gases in Mexico City**

**Award Recipient:**        **Aerodyne Research, Inc.  
45 Manning Road  
Billerica, MA 01821-3976**

**Contract No.:**        **DE-FG02-05ER63982**

**Project ID:**        **ER63982-1025333-0011046**

**Program Manager:**        **Rickey C. Petty  
Division: SC-23.3  
Phone: 301-903-5548**

**Principle Investigators:** **Dr. Charles E. Kolb, Dr. Douglas R. Worsnop**

**Other Senior Investigators:** **Dr. Manjula R. Canagaratna, Dr. Scott C.  
Herndon, Dr. John T. Jayne, Dr. W. Berk  
Knighton (Montana State University), Dr.  
Timothy B. Onasch, Dr. Ezra C. Wood, Dr.  
Miguel Zavala (Massachusetts Institute of  
Technology and Molina Center for Energy and  
Environment)**

**March 31, 2008**

## Executive Summary

This project was one of three collaborating grants designed to understand the atmospheric chemistry and aerosol particle microphysics impacting air quality in the Mexico City Metropolitan Area (MCMA) and its urban plume. The overall effort, titled MCMA-2006, focused on: 1) the primary emissions of fine particles and precursor gases leading to photochemical production of atmospheric oxidants and secondary aerosol particles and 2) the measurement and analysis of secondary oxidants and secondary fine particulate matter (PM) production, with particular emphasis on secondary organic aerosol (SOA).

MCMA-2006 pursued its goals through three main activities: 1) performance and publication of detailed analyses of extensive MCMA trace gas and fine PM measurements made by the collaborating groups and others during earlier MCMA field campaigns in 2002 and 2003; 2) deployment and utilization of extensive real-time trace gas and fine PM instrumentation at urban and downwind MCMA sites in support of the MAX-Mex/MILAGRO field measurements in March, 2006; and, 3) analyses of the 2006 MCMA data sets leading to further publications that are based on new data as well as insights from analysis and publication of the 2002/2003 field data.

Thirteen archival publications were coauthored with other MCMA-2003 participants. Documented findings included a significantly improved speciated emissions inventory from on-road vehicles, a greatly enhanced understanding of the sources and atmospheric loadings of volatile organic compounds, a unique analysis of the high fraction of ambient formaldehyde from primary emission sources, a much more extensive knowledge of the composition, size distributions and atmospheric mass loadings of both primary and secondary fine PM, including the fact that the rate of MCMA SOA production greatly exceeded that predicted by current atmospheric models, and evaluations of significant errors that can arise from standard air quality monitors for ozone and nitrogen dioxide.

Deployment of the Aerodyne mobile laboratory, equipped with instruments from five collaborating laboratories, at the T0 urban supersite, four downwind sites and the Tula industrial area yielded unique trace gas and fine PM data sets during the March 2006 MAX-Mex/MILAGRO campaign. In addition, on-road measurements as the mobile laboratory moved between sites provided extensive data on 2006 MCMA fleet averaged vehicle emissions. Analyses of 2006 data sets have yielded the identification of a close correlation between the rate of production of SOA and “Odd Oxygen” ( $O_3 + NO_2$ ) and primary organic PM with CO in the MCMA urban plume, a more sophisticated understanding of the interplay between nitrogen oxide speciation and ozone production, the identification of significant vehicular emission sources of HCN and  $CH_3CN$  (usually associated with biomass burning), characterization of the aging of primary carbonaceous PM, and updated 2006 MCMA fleet on-road trace gas and fine PM emissions.

Results from analyses of 2002/2003 and 2006 emissions and ambient measurements have conveyed to Mexican air quality managers who are using these data to devise and assess air quality management strategies. All data sets and published analyses are available to DOE/ASP researchers evaluating the impact of urban emissions on regional climate.

## 1. Introduction

The Mexico City Metropolitan Area (MCMA) is the most highly populated megacity in North America. With the pollutant emissions from daily activities of approximately twenty million inhabitants and a subtropical location it is subject to intense atmospheric photochemistry producing heavy loadings of secondary pollutants, including oxidants and aerosol particles. The overall goal of this project and the other collaborating MCMA-2006 projects was to advance our knowledge of MCMA photochemical precursor emissions and ambient processes that produce secondary pollutants, with special emphasis on secondary organic aerosol particle formation and fate. It is likely that understanding the chemistry and aerosol microphysics of Mexico City's urban atmosphere and downwind plume will help establish how the poor air quality of a developing world megacity impacts urban to regional scale human health and ecosystem viability as well as local to continental scale climate.

The project reported here was led by Aerodyne Research, Inc. (ARI) and included a subcontract to Montana State University (MSU). The ARI/MSU effort was coordinated with DOE/ASP funded collaborators at the University of Colorado at Boulder (CU) and the Massachusetts Institute of Technology/Molina Center for Energy and Environment (MIT/MCE2). This multi-institution collaboration had three tasks: 1) Analysis of extensive Mexico City air quality data sets obtained by the collaborating laboratories during the MCMA-2002/2003 field campaigns and publication of analysis results; 2) Field measurement planning and deployment in and downwind of Mexico City for MCMA-2006 field campaign, in support of the MAX-Mex/MILAGRO field campaigns in March, 2006; 3) Analysis of MCMA-2006 data and publication preparation.

The scientific goals for MCMA-2006 field measurements were to: 1) Characterize primary and secondary fine PM at the T0 urban supersite and selected downwind sites as thoroughly as possible; 2) Correlate fine PM physical properties and chemical constituents with emission tracers ( $\text{CO}_2$ , CO, NOy, NOx/NOy,  $\text{CH}_3\text{CN}$ , etc.) and precursor gases (aromatic, oxygenated and olefinic VOCs,  $\text{NH}_3$ ,  $\text{HNO}_3$ , NOy, etc.); and, 3) Compare fleet averaged motor vehicle emissions and selected ambient fine PM properties and tracer/PM precursor gases measured in MCMA-2002/2003 with those measured during MCMA-2006.

The ARI/MSU portion of the MCMA-2006 field measurement campaign deployed the ARI mobile laboratory to characterize trace gas and fine particulate matter (PM) urban source emissions and downwind urban/industrial plumes. In addition, 2006 on-road motor vehicle fleet averaged trace gas emissions were measured as the mobile lab moved between T0 and the various downwind measurement sites. The mobile laboratory carried instruments from MCE2, MSU, Virginia Polytechnic Institute (Virginia Tech), and Los Alamos National Laboratory (LANL), as well as its normal complement of real-time trace gas and fine particle instrumentation from ARI.

Contributions of the ARI/MSU team to the MCMA-2003 analysis and publication task and the MCMA-2006 deployment and subsequent analysis/publication tasks listed above were substantial. Funding from the ARI/MSU project contributed to data analyses and publication preparation activities leading to thirteen archival papers co-authored by ARI/MSU scientists presenting MCMA-2002/2003 findings. In March 2006 the ARI mobile laboratory was successfully deployed at T0, and four downwind sites, plus the Tula industrial area to the northeast of MCMA. Analyses of MCMA-2006 data have led to the submission of two manuscripts for publication and eight more are in process. In addition, collaborations with modeling groups at MCE2, the Pacific Northwest National Laboratory (PNNL), Georgia Institute of Technology (Georgia Tech), and Carnegie Mellon University (CMU) that are expected to result in further publishable analyses and data/simulation comparisons.

This project's accomplishments in performing the three MCMA-2006 team tasks listed above and its progress achieving the MCMA-2006 scientific goals are presented in the following report sections. A review of MCMA-2002/2003 data analyses and publications is presented in Section 2. Information on the deployment of the March 2006 ARI MCMA Mobile laboratory and the on-road emissions data collected during transits between sites are presented in Section 3 and progress on the analysis and publication of mobile laboratory and other data collected at various fixed sites is presented in Section 4. Section 5 presents the report's summary and publications resulting from the project and other technical references are listed in Section 6.

## 2. MCMA-2002/2003 Data Analyses and Publications

The first project goal was to expedite analyses of data and associated publications from the MCMA-2002 exploratory campaign and the MCMA-2003 major field campaign, both of which included extensive deployment of the Aerodyne mobile laboratory for both on-road and multiple fixed site deployments. Thirteen publications based on these analyses are listed in Section 6.1 below. One was published in 2005, seven in 2006 and four in 2007, some in time to support planning for the March 2006 MAX-Mex/MILAGRO deployments and all in time to inform most detailed data analyses of the 2006 measurements and preparation of publications of Max-Mex/MILAGRO campaign results. All of these papers resulted from close collaborations with a range of U.S. and, often, Mexican research groups that participated in the MCMA-2002/2003 measurements.

Two of the articles listed in Section 6-1 present analyses on-road emissions obtained by deploying the Aerodyne mobile lab on a wide range of MCMA roads in both chase mode (where only intercepted exhaust plumes from specific target vehicles are analyzed to produce emissions data for selected vehicle classes) and fleet average mode, where all on-road intercepted exhaust emission data are included. Paper 1 (Jiang et al., 2005) analyzed on-road data from relatively slow response ( $>10$ s) instruments to produce vehicle emission inventories for black carbon, particle bound polycyclic hydrocarbons (PAHs), hydrocarbons, CO and NO<sub>x</sub>. Paper 7 (Zavala et al., 2006) presented on-road emission ratios to exhaust CO<sub>2</sub>, which allow the calculation of fuel based emission indices and total annual emissions for a variety of gaseous exhaust species, including: NO, NO<sub>2</sub>, NO<sub>y</sub>, NH<sub>3</sub>, HCHO, CH<sub>3</sub>CHO, benzene, toluene, and selected aromatic VOC classes for a full range of major vehicle classes at various on-road speed intervals. These papers form the basis of a re-evaluation on on-road vehicle emission inventories for the MCMA that have subsequently been utilized as input for more accurate photochemical models of the MCMA atmosphere.

The Zavala et al. paper revealed very high levels of HCHO and CH<sub>3</sub>CHO emissions from the MCMA fleet, providing a major source of early morning radicals to “jump-start” the city’s photochemistry. This topic was further addressed in paper 4 (Garcia et al., 2006), which used ambient glyoxal concentrations, as novel tracer of photochemical activity, along with CO, an exhaust emissions tracer, to estimate that primary (vehicular) emissions were responsible for as much ambient HCHO near within the MCMA urban core as the well known photochemical secondary HCHO source. Paper 9 (Velasco et al., 2007) aggregated mobile laboratory real-time and canister sampled VOC measurements with similar data from a central fixed site to assess the concentration and spatial distributions, diurnal patterns and reactivities of ambient VOCs, allowing an insightful evaluation of the VOC emission inventories for the MCMA. Again this work is critical for assessing and choosing accurate inputs for photochemical models to evaluate and explain MCMA air quality.

Papers 2, 10 and 12, present and analyze high time resolution Aerodyne AMS measurements of the MCMA fine particle composition along with additional PM

measurements. They establish that daytime fine PM loadings are dominated by secondary inorganic and organic material, with important contributions from ammonium nitrate, ammonium sulfate and, sporadically ammonium chloride, but even larger contributions from SOA. Papers 5 and 6 use a novel inverse algorithm to model the equilibrium chemistry the inorganic secondary aerosol species listed above with their precursor gases, predicting concentrations for precursors that were not measured and comparing predictions with data for these that were. Paper 8 established the critical fact that the observed formation of MCMA SOA was both much faster and more extensive than current mechanisms in photochemical models allow.

Papers 2 and 11 document how standard air quality monitors for the criteria pollutants, O<sub>3</sub> and NO<sub>2</sub>, can fail in the heavily polluted MCMA atmosphere. Paper 13 presents an overview of all of the published accomplishments of the MCMA-2002/2006 team.

### 3. Overview of the deployment of the Aerodyne mobile laboratory in the MCMA-2006 field campaign

The Aerodyne mobile laboratory was deployed in Mexico City in support of the MCMA-2006/MAX-Mex/MILAGRO field campaigns. The mobile laboratory deployed a comprehensive set of research grade, real-time trace gas and fine particulate matter instruments at six representative urban and boundary sites across the Mexico City Metropolitan Area (MCMA). Figure 3-1 shows the location of the monitoring sites where the ARI mobile laboratory was deployed. By providing more diverse spatial coverage beyond the MILAGRO supersites (T0, T1, and T2), the deployment of the mobile laboratory provided a large set of additional valuable information on the characteristics of trace gases and aerosols and downwind of the city. These comprehensive datasets, in combination with other measurements made during the MILAGRO campaign, will serve

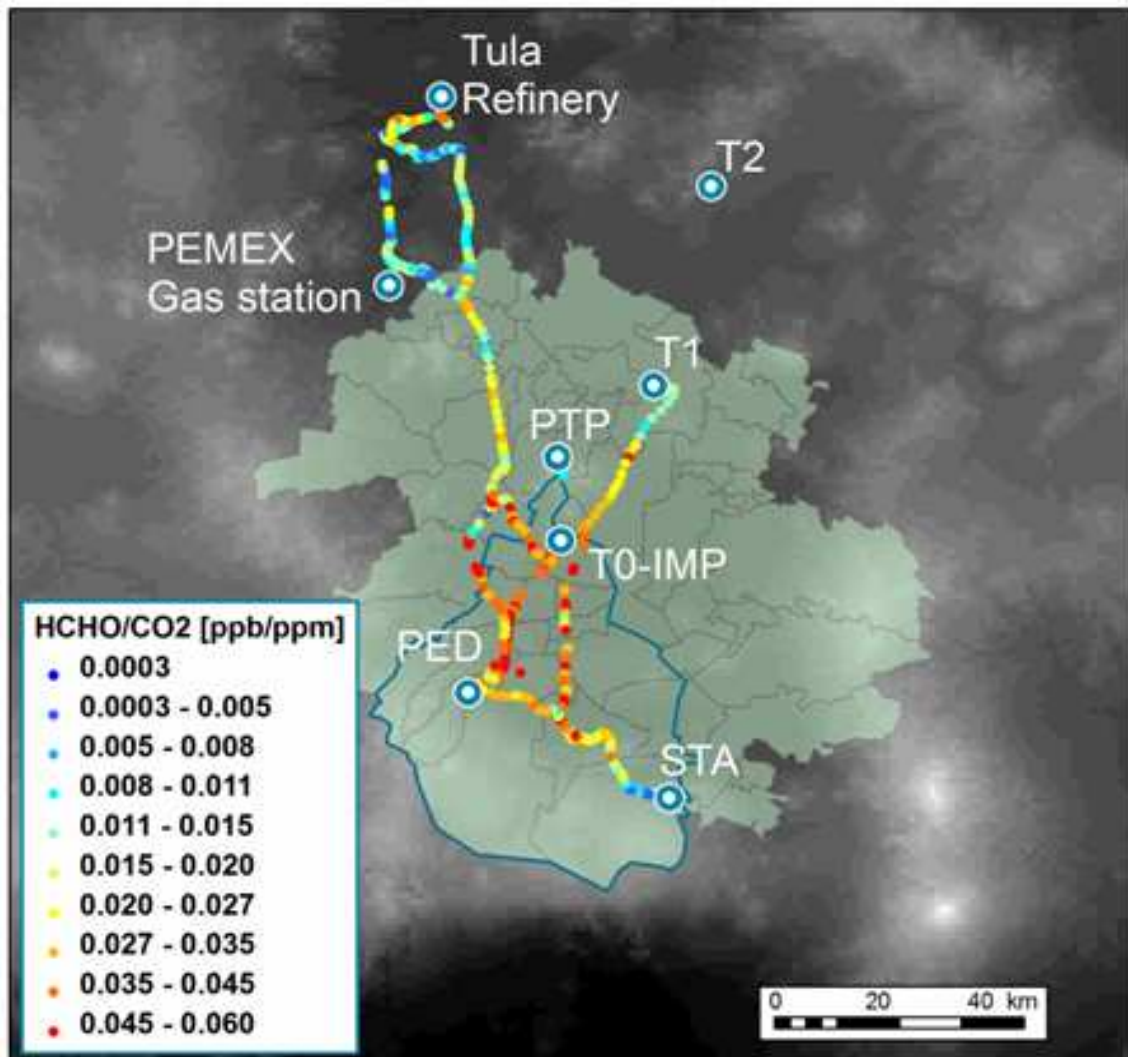


Figure 3-1. Monitoring sites where the Aerodyne mobile laboratory was deployed. Also shown, on-road ratios of H<sub>2</sub>CO/CO<sub>2</sub> [ppb/ppm].

as an important basis for understanding the physical and chemical processes that characterize the air pollution phenomena in the MCMA and similar megacities. In addition, the rich database provides a unique opportunity for investigating relevant research questions on the regional and global impacts of air pollution from megacities to ecosystems and our climate.

A description of the mobile lab monitoring sites is presented in Table 3-1. The downwind monitoring sites were selected in advance on the basis of experiences in prior missions and on daily wind forecasts produced by Benjamin de Foy (MCE2) and Jerome Fast (PNNL), in consultation with Sasha Madronich of the National Center for Atmospheric Research (NCAR) and Luisa Molina (MCE2). Since the mobile lab has the capabilities of rapid deployment and mobility, urban plume measurements were less limited by the prevailing meteorological conditions, in contrast to fixed measurement sites. The measurements obtained by the mobile lab were designed a priori (e.g. moving downwind into the city's emissions outflow, or of specific industrial emissions, capturing channel inflow to the city, or obtaining basin background conditions). Valuable logistic support at several sites was provided by Rafael Ramos-Villegas, Director of the Red Automática de Monitoreo Atmosférico.

In addition to the stationary site measurements, the fast response instrumentation was also used during mobile lab transits between sites to obtain on-road vehicle emissions data. These measurements, taken under fleet-average sampling conditions using the analysis technique described in Zavala et al., (2006), will better characterize the emissions from mobile sources in the city. MCMA mobile emission sources produce a significant fraction of the total anthropogenic emissions burden in the city. It is, therefore, very important to validate the bottom-up model-based official estimates of mobile emissions from the emissions inventory (CAM, 2006) with actual on-road fleet emission measurements. The on-road emissions measurements taken by ARI during MILAGRO are being used to evaluate the uncertainties involved in estimating these emissions. By comparing with previous mobile lab measurements taken in 2002 and 2003 MCMA field campaigns, the mobile emissions data collected in 2006 will help characterize the evolution of these important emission sources. Figure 3-2 shows a comparison of selected key on-road VOC's emission ratios (exhaust pollutant (ppb/exhaust CO<sub>2</sub> (ppm))) from the gasoline fleet obtained in Mexico City in 2003 and in 2006 during MILAGRO.

One manuscript (Thornhill et al., 2007) describing particulate polycyclic hydrocarbon distributions made at several MCMA mobile laboratory deployment sites has been submitted for publication (see Section 6.2).

Currently, three papers are being prepared for submission describing the mobile lab deployment modes and on-road measurements during MILAGRO. These are:

**(1) Deployment of the Aerodyne mobile laboratory during the MILAGRO/MAX-Mex/MCMA-2006 field campaign, M. Zavala et al.**



(2) Evolution of on-road emissions from mobile sources in Mexico City, M. Zavala et al.

(3) Application of positive matrix factorization to on-road gaseous and particulate measurements for source apportionment of diesel and gasoline vehicle emission in Mexico City, D. Thornhill et al.

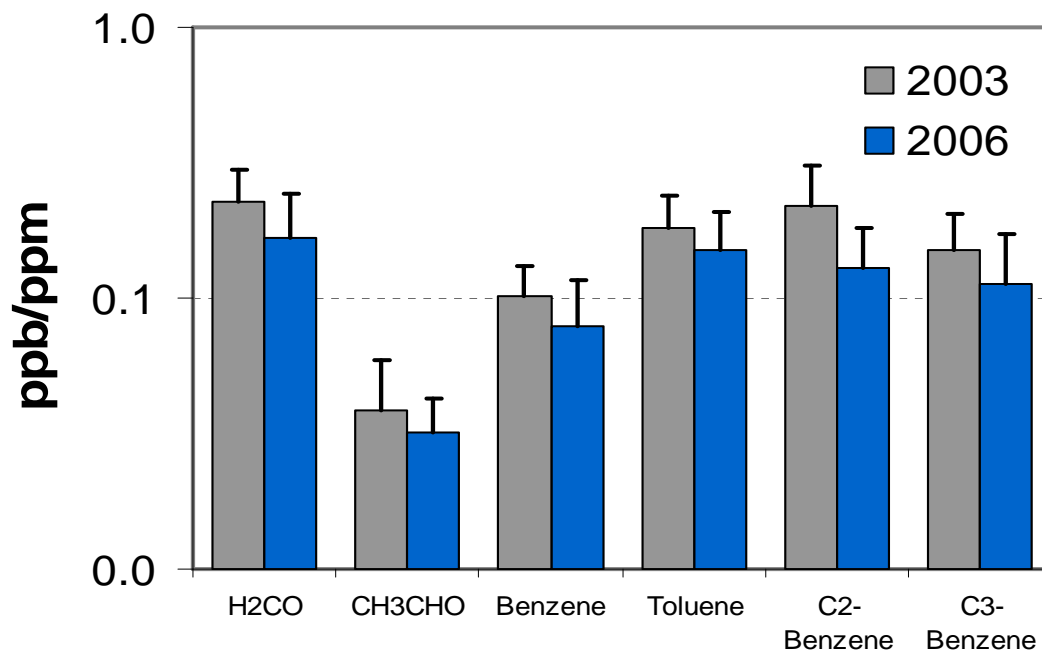









Figure 3-2. Comparison of selected key on-road VOC exhaust emission ratios [pollutant ppb/ CO<sub>2</sub> ppm] from the gasoline fleet obtained by ARI in Mexico City in 2003 and in 2006 during MILAGRO.

Table 3-1. Description of measurement sites where the Aerodyne mobile lab was deployed during the MILAGRO field campaign

Site	Site view	Period	Site
<b>T0</b>		3/01/06 - 3/04/06 3/06/06 - 3/07/06 3/27/06 - 3/31/06	Urban site near the center of the city with homogenous mixture of mobile, domestic and industrial emissions. Altitude: 2236 m
<b>PED (Pedregal)</b>		3/04/06 – 3/06/06	Urban site with predominance of mobile and domestic emissions. Potential “receptor” site. Altitude: 2334 m
<b>PTP (Pico de Tres Padres)</b>		3/07/06 – 3/19/06	Top of the mountain site located in the middle of the city. No influence of local anthropogenic emission sources. Altitude: 2991 m
<b>T1 (Tecamac)</b>		3/19/06 – 3/22/06	Semi rural semi-arid site in the Northeast with periods of influence from local town (Tecamac) and MCMA emissions. Altitude: 2259 m
<b>STA (Santa Ana)</b>		3/22/06 – 3/25/06	Rural site in the southwest part of the city. Depending on meteorology it is a potential “receptor” site or representative for boundary conditions. Altitude: 2591 m
<b>PEMEX ( Near Tula)</b>		3/25/06 – 3/27/06	Gas transfer station located in the Northwest of the city. Potential “receptor” site for nearby industrial emissions. Altitude: 2306 m
<b>Mobile/ Tula</b>		Between sites	Sampling during mobile lab transits between sites and for “transect” experiments in the Tula region.

## 4. Fixed site measurements and analyses

During MILAGRO 2006, the Aerodyne Mobile Laboratory made measurements at several fixed sites within the greater Mexico City Metropolitan Area, including the T0 and T1 supersites; Pedregal and Santa Ana which are both south of the city; Tula an industrial area north of the MCMA; and Pico de Tres Padres (PTP), which is a mountain-top site located in between MILAGRO measurement sites T0 and T1 (Figure 4-1).

### 4.1 Analyses of organic aerosol composition

For each of the measurement sites listed above positive matrix factorization (PMF) was applied to the fine particulate matter data collected by the Aerodyne aerosol mass spectrometer (AMS). This and related techniques have been successfully used in other

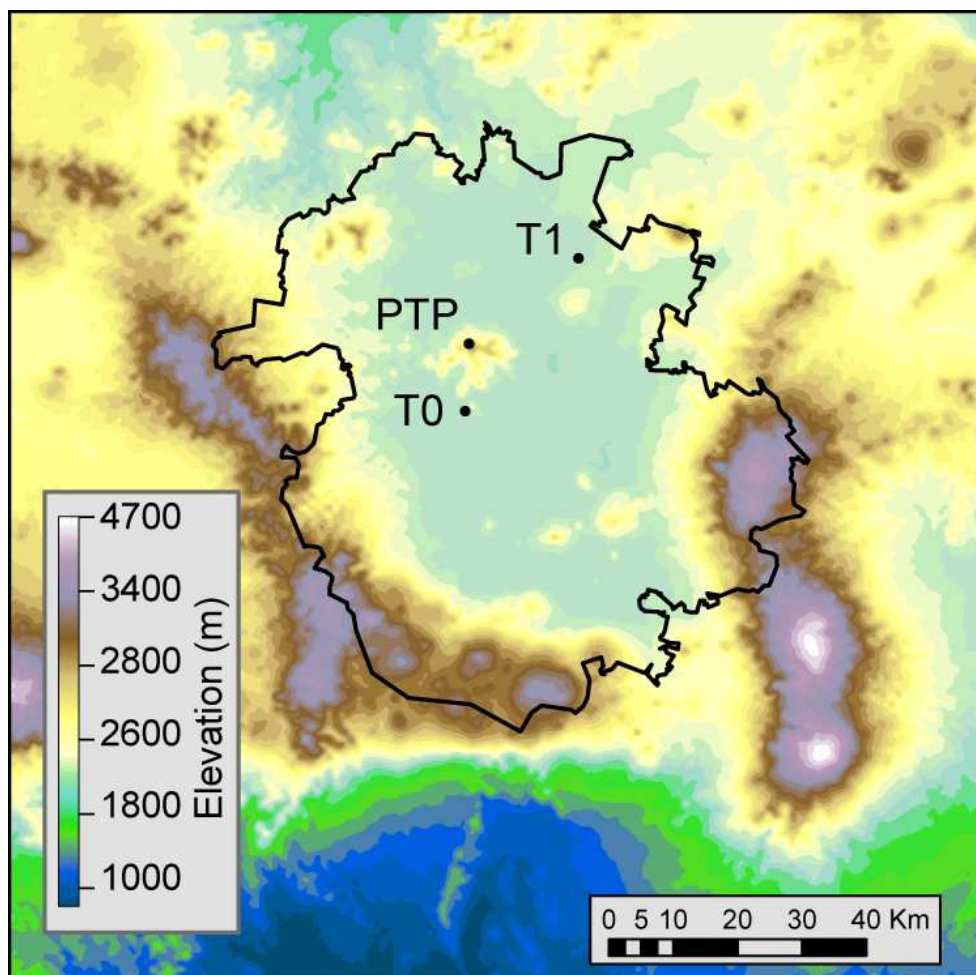


Figure 4-1. Topography of the Mexico City Metropolitan Area. The site labeled “PTP” is an elevated location within the defined city limits.

fine aerosol composition studies (Lanz et al., 2007; Volkamer, et al., 2006; Zhang, et al., 2007; Zhang, et al., 2005) to glean insight into the distribution of organic aerosol (OA) between primary organic aerosol (POA) and secondary organic aerosol (SOA), the latter of which is currently poorly described by atmospheric chemistry models.

The PTP site was particularly useful for such analyses due to its unique positioning, approximately 700 m above the elevation of the city, and because it is only minimally affected by nearby emissions. At night this measurement site was frequently above the nocturnal boundary layer allowing regional background aerosol characterization. A time series of several pollutants at PTP is shown in Figure 4-2. The hydrocarbon-like organic aerosol (HOA) component of the total OA measurement is tightly correlated with the primary pollutants CO, black carbon, and  $\text{NO}_y$  (the sum of all oxidized nitrogen species) suggesting that it is a good proxy for POA. The oxidized organic aerosol component (OOA) is strongly correlated with the secondary pollutants  $\text{O}_x$  (“odd-oxygen”), the sum of  $\text{O}_3$  and  $\text{NO}_2$ , and  $\text{NO}_z$ , the oxidation products of  $\text{NO}_x$ ; suggesting that OOA is a good proxy for SOA. The correlation of  $\text{O}_x$  with OOA is shown in Figure 4-3. For comparison, data from a high-ozone episode observed in La Porte, TX ( near Houston) during the 2000 Texas Air Quality Study is included in the figure.

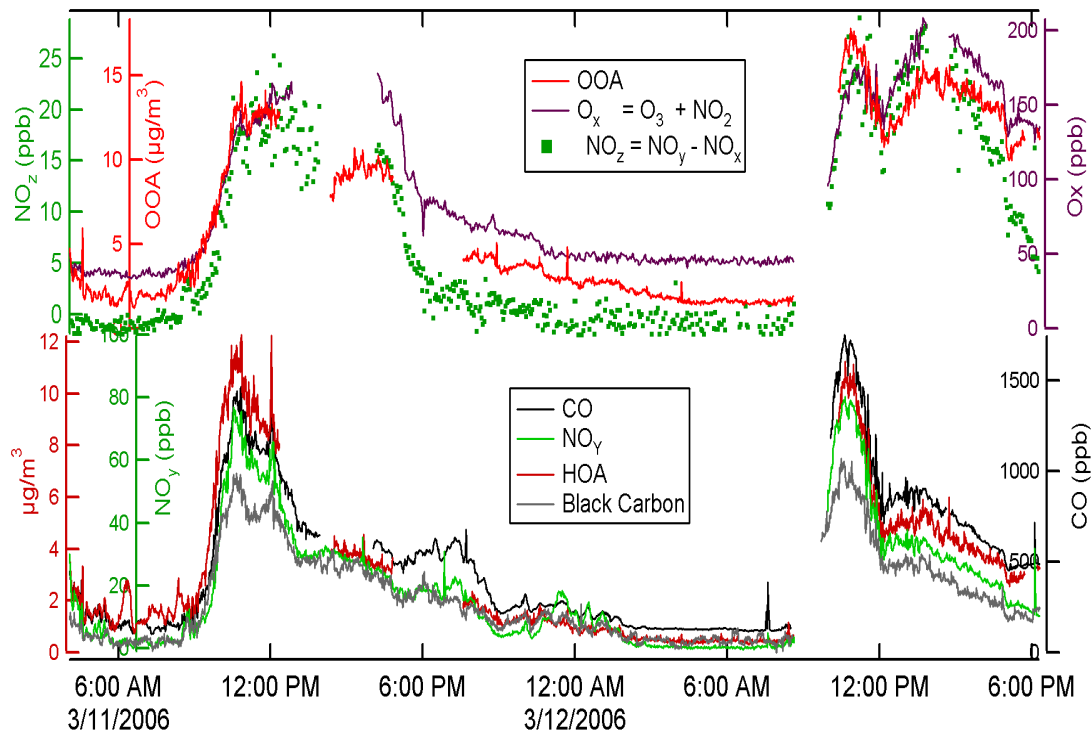


Figure 4-2. Time series of OOA,  $\text{O}_x$ ,  $\text{NO}_z$ , CO,  $\text{NO}_y$ , HOA, and black carbon at Pico de Tres Padres on March 11 and 12, days which were characterized by relatively stagnant air during the afternoon. OOA correlates well with the secondary pollutants  $\text{O}_x$ , and  $\text{NO}_z$ , whereas HOA correlates well with the primary pollutants CO,  $\text{NO}_y$ , and black carbon.

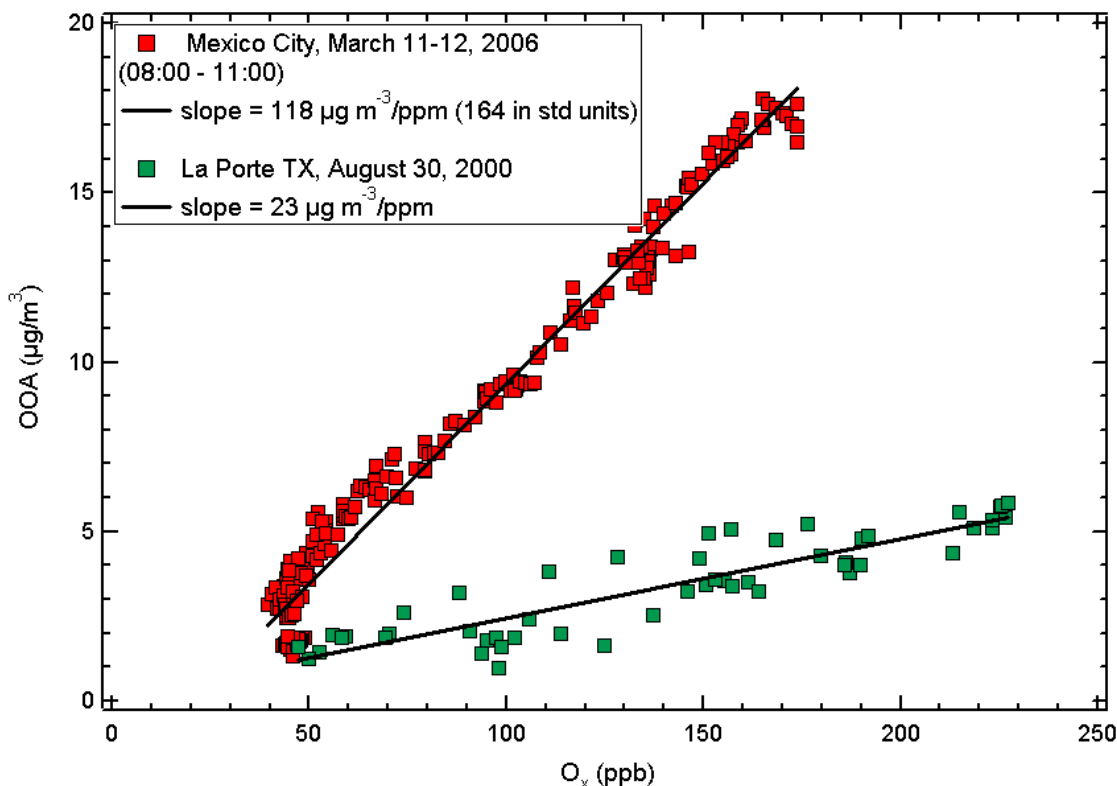


Figure 4-3. Correlation of OOA with O<sub>x</sub> observed during the morning (08:00 – 11:00 CST) at PTP on March 11 and 12, 2006 and the entire day at La Porte, TX 8/30/2000. The VOCs contributing to O<sub>x</sub> and SOA production in PTP come mainly from vehicular sources, while the VOCs at La Porte on this day were heavily influenced by very high concentrations of ethene and propene from the nearby petrochemical facilities.

The correlation between O<sub>x</sub> and OOA suggests that the wealth of knowledge gained by studies of photochemical ozone production over the last several decades will be useful in analyzing the extent of SOA formation. Atmospheric models are reasonably good at predicting ozone concentrations, usually to well within a factor of two, but very poor at predicting SOA concentrations (Volkamer et al., 2006). Ozone formation and secondary aerosol formation are fundamentally linked since they are both initiated by the oxidation of volatile organic compounds (VOCs).

The ozone (or O<sub>x</sub>) production rate can be equated to the rate at which peroxy radicals are produced by the oxidation of VOCs (Kleinman, 2005). Using this approach, we have compared the calculated production rate of O<sub>x</sub> using VOCs measured on board the mobile laboratory by quantum cascade tunable infrared laser differential absorption spectrometry, proton transfer mass spectrometry, and whole canister sample analyses. The production rate of SOA has been expressed in a similar manner, based on VOC oxidation rates and SOA formation yields measured in previous laboratory studies. Since O<sub>x</sub> and OOA are both long-lived, this ratio of production rates is expected to mirror the observed concentrations of both species if the current understanding of secondary organic aerosol formation is correct.

As anticipated, the model predicted ratio of OOA/O<sub>x</sub> underestimates the observed ratio by an order of magnitude, similar to previous studies (de Gouw et al., 2005; Heald et al., 2005; Volkamer et al., 2006). However, several factors do yield insight into the missing SOA formation mechanisms: 1) the extent of disagreement; 2) the variation in these quantities with photochemical aging; and 3) the comparison between Mexico City and Houston. This analysis has suggested that a large portion of total SOA is the result of the oxidation of VOC precursors that are not commonly measured by current analytical equipment and are oxidized more rapidly than conventional ozone precursor VOCs (i.e., light alkenes, aromatics, CO, alkanes, and oxygenated VOCs). A manuscript describing the results of SOA formation analysis at PTP (Herndon et al., 2008) has been submitted to Geophysics Research Letter (see Section 6.2).

A second manuscript presenting similar analysis for a range of MCMA measurement sites with a comparison to Houston is in preparation:

**Wood E. et al., Quantitative Investigation of the Correlation between odd-oxygen and secondary organic aerosol in Mexico City and Houston.**

## **4.2 Analysis of urban plume ozone – NO<sub>y</sub> – HO<sub>x</sub> relationship**

Observations of a stagnant air mass at Pico de Tres Padres (a mountain-top site within the Mexico City basin) were used to characterize ozone production, the reactive nitrogen budget, and the flux of radicals in the Mexico City urban plume. Numerous quantities have been derived to test predictions from atmospheric chemistry models, including the instantaneous ozone production rates, its relationship to HO<sub>x</sub> radical production rates, the ozone production efficiency of NO<sub>x</sub>, and the speciation of nitrogen oxides.

The *net* ozone production rate (ie, the sum of the production and destruction rates) was calculated by the time increase in O<sub>x</sub> during a stagnant period of time in the afternoon, when CO mixing ratios were relatively invariant and wind speeds were less than 1 m/s. The total ozone production rate during this time period was ~45 ppb/hr, which is among the highest observed anywhere in the world (Kleinman, et al., 2005). The largest loss mechanism of O<sub>x</sub> was the oxidation of NO<sub>2</sub> to more highly oxidized nitrogen oxides such as nitric acid (HNO<sub>3</sub>) and organic nitrates.

The speciation of NO<sub>y</sub> in this stagnant air mass was markedly different than that measured in other locations across the world. Gas-phase HNO<sub>3</sub> accounted for less than 10% of total NO<sub>z</sub> (NO<sub>z</sub> = NO<sub>y</sub> – NO<sub>x</sub>), and particulate nitrate (measured with an aerosol mass spectrometer) accounted for 20% to 50% of NO<sub>z</sub> (Figure 4-4). This high ratio of aerosol nitrate to gas-phase HNO<sub>3</sub> is mostly due to the high ambient concentrations of ammonia (NH<sub>3</sub>). The remaining contributors to NO<sub>z</sub> were unmeasured, though are most likely organic nitrates. Over 80% of NO<sub>x</sub> had been oxidized to these various NO<sub>z</sub> species

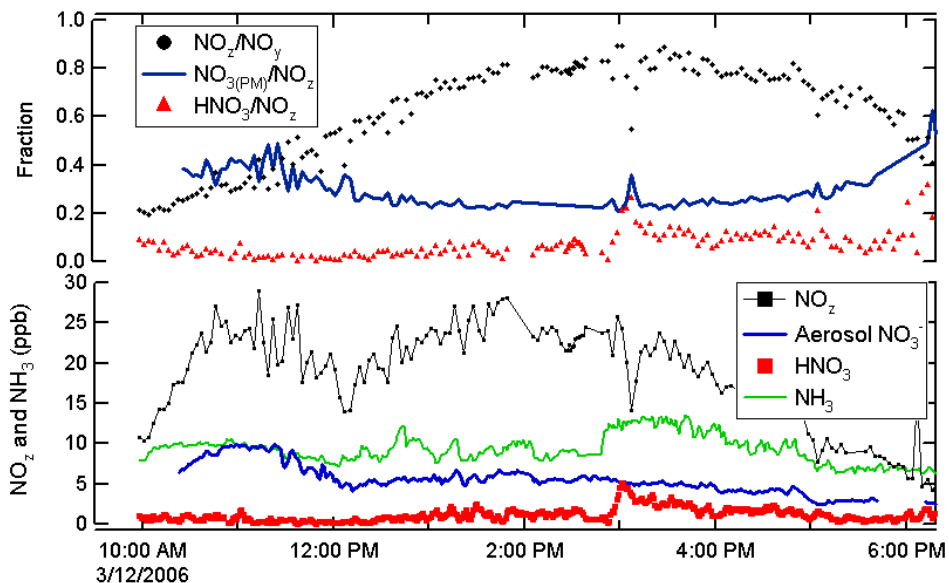


Figure 4-4. Partial speciation of  $\text{NO}_y$  at PTP. Aerosol nitrate accounts for 20-40% of  $\text{NO}_z$  during the day, and  $\text{HNO}_{3(\text{g})}$  accounts for less than 10%.  $\text{NH}_{3(\text{g})}$  is included for comparison, though is not a part of  $\text{NO}_y$  or  $\text{NO}_z$ . The high  $[\text{NH}_3]/[\text{HNO}_3]$  ratios (3.5 to over 100) result in the high ratios of  $[\text{NO}_3^-(\text{PM})]$  to  $[\text{HNO}_3]$ .

after 6 hours of atmospheric oxidation. Estimates of the  $\text{HNO}_3$  and particulate nitrate formation rate using measurements of  $\text{NO}_2$  and estimates of  $[\text{OH}]$  indicate that  $\text{HNO}_3$  formation (and by extension particulate nitrate) can only account for 20% - 40% of the observed  $\text{NO}_z$  production rate during the afternoon. This speciation is in agreement with those measured aboard the C130 aircraft (Flocke, 2008) and at the T1 supersite (Farmer, 2008).

Ozone production was VOC-limited during the afternoon, inferred by a comparison of the  $\text{RO}_x$  ( $\text{RO}_x = \text{OH} + \text{HO}_2 + \text{RO}_2$ ) production rate calculated using measured precursor compounds and the  $\text{RO}_x$  loss rate inferred from the formation of  $\text{NO}_z$  compounds (Figure 4-5). Photolysis of formaldehyde was the single greatest  $\text{RO}_x$  source, followed by the reaction of  $\text{O}(^1\text{D})$  with water vapor (following photolysis of  $\text{O}_3$ ), ozonolysis of alkenes, and photolysis of acetaldehyde. The calculated  $\text{RO}_x$  production rates were highest at 11:00 due to a “burst” of oxygenated VOC concentrations (i.e., formaldehyde, acetaldehyde, and acetone), which are all emitted directly in Mexico City (Zavala et al., 2006) (and at higher emission rates than in the US (Kolb et al., 2004)) and formed from the oxidation of VOCs. Since all the major  $\text{NO}_z$  compounds are formed by the reaction of  $\text{OH}$ ,  $\text{HO}_2$ , or  $\text{RO}_2$  with  $\text{NO}_x$ , the  $\text{NO}_z$  production rate is equal to the  $\text{RO}_x$  loss rate when ozone production is VOC limited. The calculated production rate of  $\text{RO}_x$  during the stagnant afternoon period was  $2.0 \pm 0.5$  ppt/s, which is within the uncertainties of the  $\text{NO}_z$  production rate ( $1.8 \pm 0.2$  ppt/s). This indicates that ozone production was limited by the availability of VOCs, in agreement with recent modeling work (Lei et al., 2007).



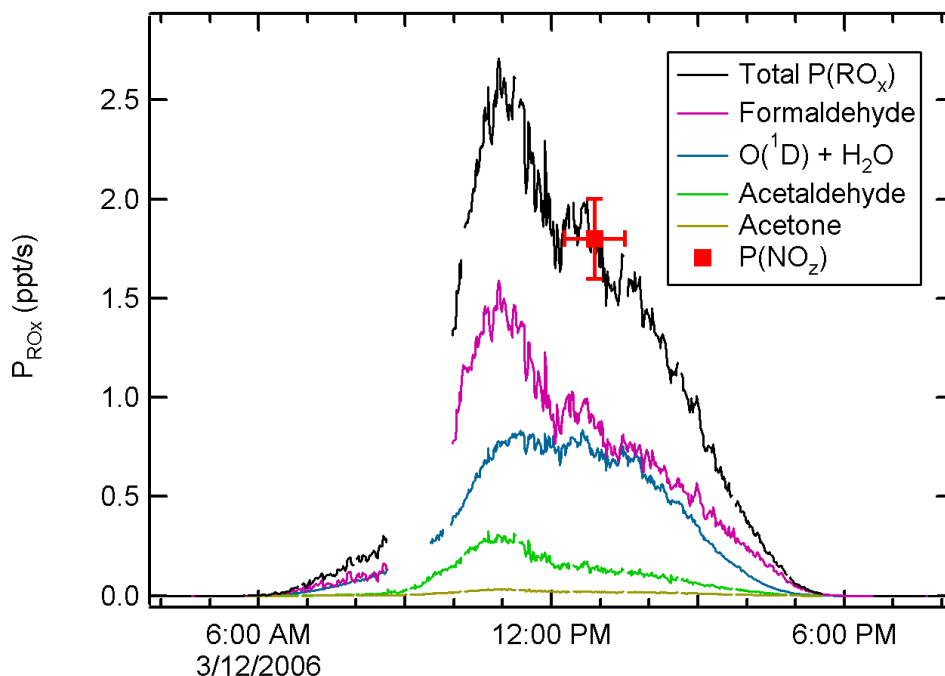


Figure 4-5. Comparison of calculated  $\text{RO}_x$  production rates and the observed  $\text{NO}_z$  production rate. Ozonolysis of VOCs contributes an additional  $0.25 \pm 0.2$  ppt/s during the afternoon. The  $\text{NO}_z$  production rate observed during the stagnant air mass between 12:15 – 13:30 is equal to the  $\text{RO}_x$  production rate within the total uncertainties, indicating that the loss mechanism for  $\text{RO}_x$  species is dominated by reactions with  $\text{NO}_x$  and not self reactions. This indicates that ozone production is VOC-limited. The red cross demarks the uncertainty in  $\text{P}(\text{NO}_z)$  and the time period during which  $\text{P}(\text{NO}_z)$  was calculated.

Since ozone production is VOC-limited and at times less than half of the  $\text{NO}_z$  can be accounted for by  $\text{HNO}_3$  and particulate nitrate, we have concluded that formation of organic nitrates represents a significant, and at times a dominant, sink for  $\text{RO}_x$  radicals.

The ozone production efficiency is defined as the number of ozone molecules that each  $\text{NO}_x$  molecule catalyzes the production of. Given that thermally labile peroxy nitrates presumably constitute a large fraction of total  $\text{NO}_x$  removal processes and can be transported large distances, the true OPE of  $\text{NO}_x$  emitted in Mexico City is not accurately expressed in a single number, and is best defined in the context of a stated time scale. The “short-term” ozone production efficiency of  $\text{NO}_x$  observed at PTP was  $5 \pm 0.5$ , inferred by the quantity  $\Delta\text{O}_3/\Delta\text{NO}_z$ , and corrected for losses of both  $\text{O}_3$  and  $\text{NO}_z$ .

The following manuscript is in preparation:

**Wood, E. et al., Nitrogen Oxides, Radical Budgets, and Ozone Production in Mexico City: Observations from Pico De Tres Padres.**



### 4.3 Characterization of urban HCN and CH<sub>3</sub>CN emissions

During the 2006 field campaign, wildfires burned throughout the area and a central question has arisen as to what extent did these fires influence the air quality the Mexico City basin. In an attempt to address this question traditional biomass burning tracers have been employed and were used to quantify the contribution of the aerosol burden within the city as a result of these fires (Yokelson et al., 2007; Kleinman et al., 2008). While it is generally accepted from a global perspective that biomass burning is a dominant source of HCN and CH<sub>3</sub>CN, biogenic and urban/industrial sources are also recognized to have significant contributions (Shim et al., 2007). In addition several studies have now identified vehicle exhaust as an emission source of HCN (Karlsson, 2004; Baum et al., 2007), which raises the question as to uniqueness these traditional tracers in an urban environment. There is a clear need to examine the extent to which HCN and CH<sub>3</sub>CN emissions originate from vehicular and other urban sources. The PTR-MS that was deployed on the Aerodyne Mobile Laboratory during the 2006 MCMA campaign did not normally monitor for these compounds, but did collect a limited set of full mass spectral scan data over the entire campaign period from which concentration data can be extracted. A series of experiments were conducted over the funding period to quantify the HCN and CH<sub>3</sub>CN concentrations from these PTR-MS responses and to determine if these compounds are emitted from vehicular or other urban sources.

Both HCN and CH<sub>3</sub>CN have proton affinities (PA) greater than that of water and thus can be detected by the PTR-MS technique. However, because the PA of HCN is only 20 kJ/mole greater than that of water the PTR-MS response to this compound is diminished because of the reverse reaction of protonated HCN with ambient water (Spanel et al., 2004). Figure 4-6 illustrates the influence of humidity (monitored as ratio of the proton hydrates) and temperature has on the measured detection efficiency. We recently developed a method, as shown in Figure 4-7, to calibrate the response of a PTR-MS to HCN using the measured H<sub>3</sub>O<sup>+</sup> and H<sub>3</sub>O<sup>+</sup>(H<sub>2</sub>O) ion signals to compensate for any changes in the HCN detection efficiency with humidity and temperature. The CH<sub>3</sub>CN concentration has been quantified using traditional PTR-MS methods (Rogers et al., 2006) and assumes a proton transfer reaction rate of  $4.7 \times 10^{-9}$  ml molecule<sup>-1</sup>sec<sup>-1</sup>.

The Aerodyne mobile lab (AML) was stationed at the T0 supersite for the last 3 days of the field campaign and Figure 4-8 shows the times series measurements for HCN, CH<sub>3</sub>CN, and the combustion dilution tracer CO. The T0 supersite is located within the urban core of Mexico City and the air at this facility is heavily impacted by both industrial and vehicular emissions. This figure clearly indicates that the HCN and CH<sub>3</sub>CN concentrations follow the same temporal profile as CO. While the elevated CO concentrations are predominately from vehicle emissions the coincident correlation of HCN and CH<sub>3</sub>CN does not definitively prove that these compounds are produced by vehicles. If the air is well mixed these signals could be from regional fire emissions that were transported into the city or from biomass and/or charcoal burning within the city.

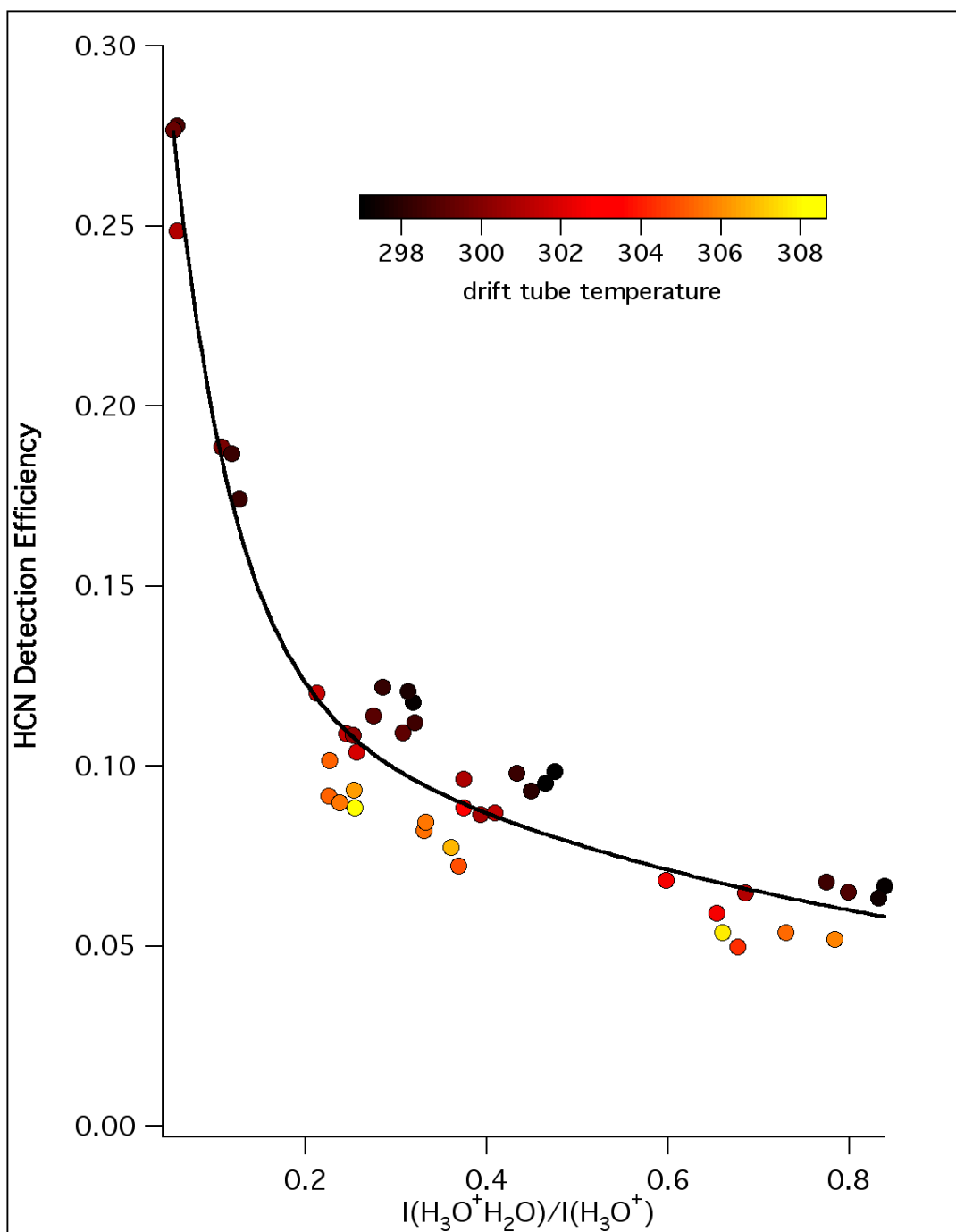


Figure 4-6. Influence of temperature and humidity on the PTR-MS response to HCN.

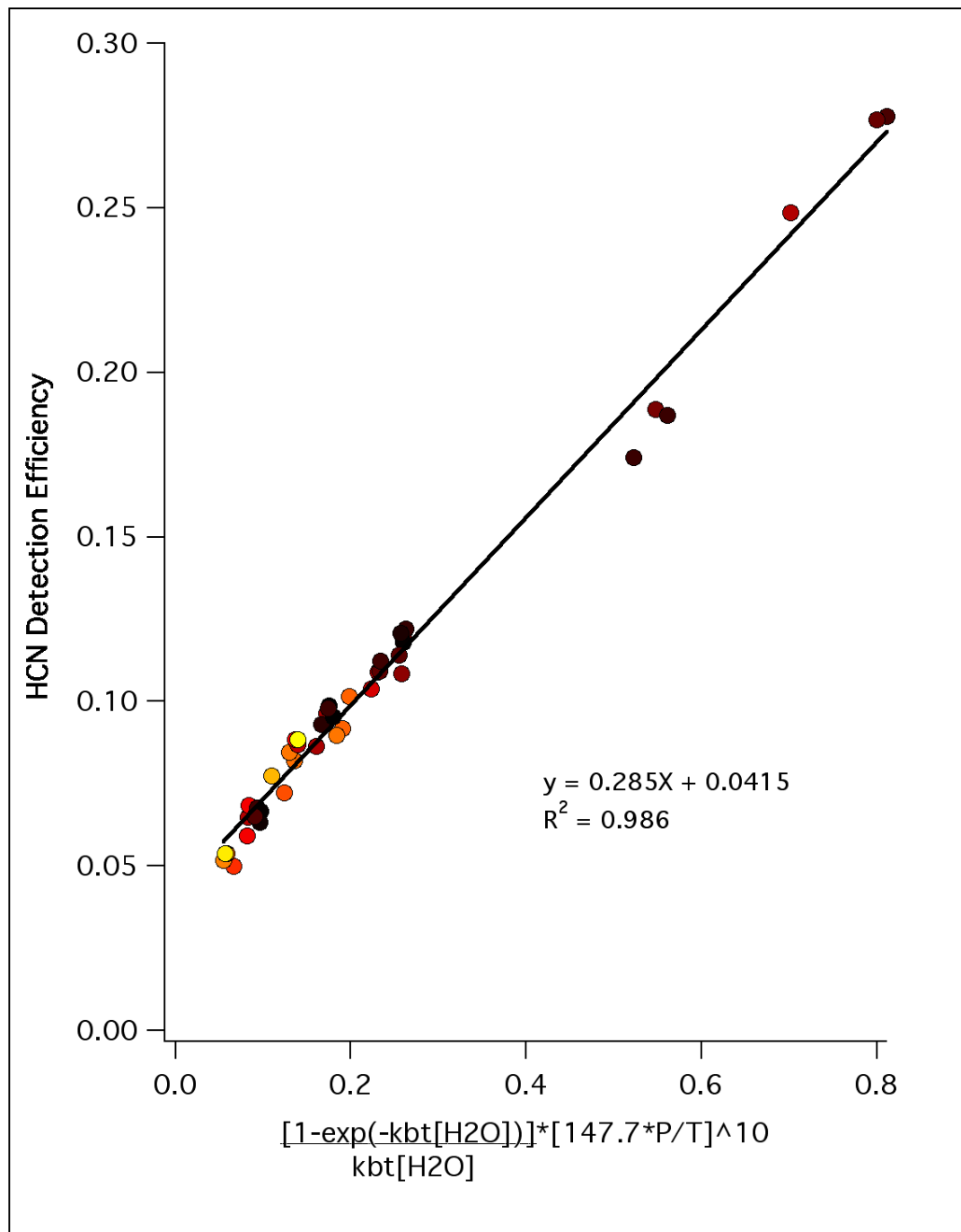


Figure 4-7. Temperature and humidity compensated response function to HCN.

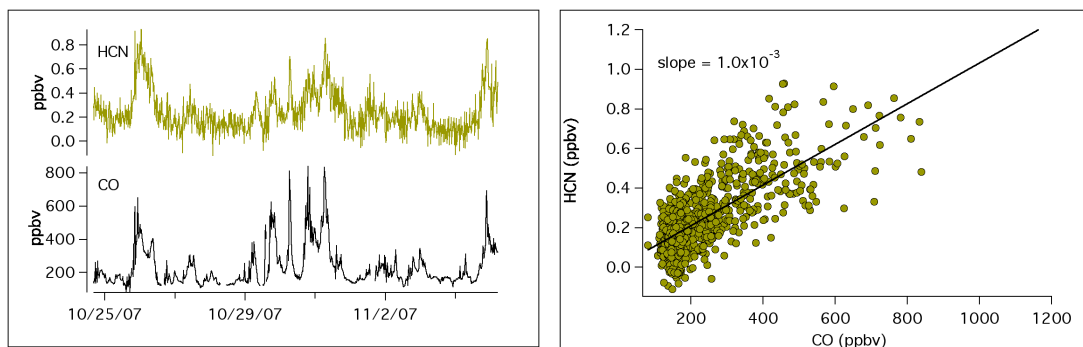


Figure 4-8. Ambient concentration measurements and correlation scatter plots of HCN and CH<sub>3</sub>CN vs CO observed at the T0 urban Mexico City supersite.

Ideally on-road studies would have been conducted during the MCMA-2006 field campaign to quantify the emissions of HCN and CH<sub>3</sub>CN in vehicle exhaust. Because these experiments were not performed in Mexico, two impromptu studies, a two-week stationary and a one-day on-road, were conducted in the greater Boston metropolitan area to determine if HCN and CH<sub>3</sub>CN are present in vehicle exhaust emissions. The PTR-MS was shipped to Aerodyne Research Inc. and was setup in the AML. For the stationary measurements the AML was parked at Aerodyne Research Inc. facility, which is located in a small technical park in the suburban Boston area. A major commuter highway lies 140 meters to west of the facility and vehicular emissions are an important, and often dominant, source of CO in this area. In January 2008, a one-day on-road experiment was conducted in the metro Boston area, on a very cold morning with low winds during and after the morning rush hour period.

Figure 4-9 shows the HCN and CO concentrations measured the ARI suburban Boston location. CH<sub>3</sub>CN measurements have not been included because one of businesses occupying the technical park utilizes this compound as a solvent. The HCN and CO time series measurements are correlated and HCN/CO emission ratio is slightly greater than that observed in Mexico City. The similarity in the emission ratios observed in Mexico City to that in suburban Boston implies that vehicle exhaust emissions are the predominate source of HCN. Fire emissions should not be important as no significant biomass or trash burning events were occurring within the region. Further support for the conclusion that HCN and CH<sub>3</sub>CN are components of vehicle exhaust is provided from the on-road study. Figure 4-10 shows the on-road time series measurements for these components. For these on-road measurements the excess CO reflects the sampling of vehicle exhaust plumes and the coincident change in the HCN and CH<sub>3</sub>CN signals provides direct evidence of the co-emission of these compounds.

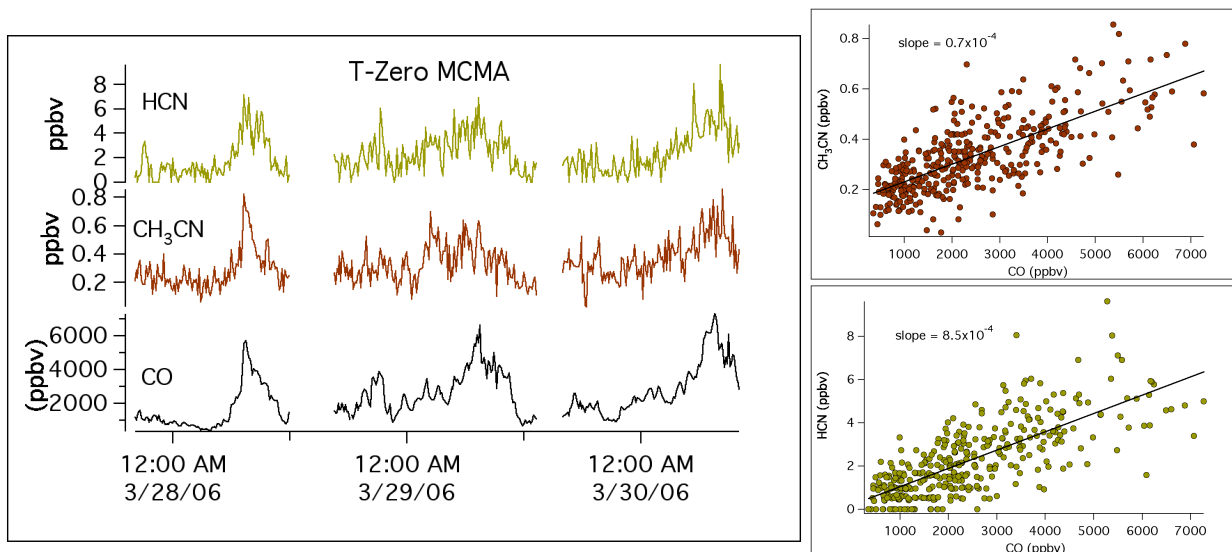


Figure 4-9. Ambient concentration measurements and the correlation scatter plot of HCN vs CO observed at ARI facility located 20 miles northwest of Boston MA.

The presence of HCN or  $\text{CH}_3\text{CN}$  in vehicle exhaust has been clearly demonstrated. This suggests that these compounds should not be interpreted as biomass tracer compounds in urban air masses unless there is evidence of persistent fire sources that swamp vehicular emissions.

The two manuscripts noted below are in preparation:

**Knighton, W. B et al., HCN detection with a proton transfer mass spectrometer.**

**Knighton, W. B et al., Characterization of MCMA urban HCN and  $\text{CH}_3\text{CN}$  emissions.**

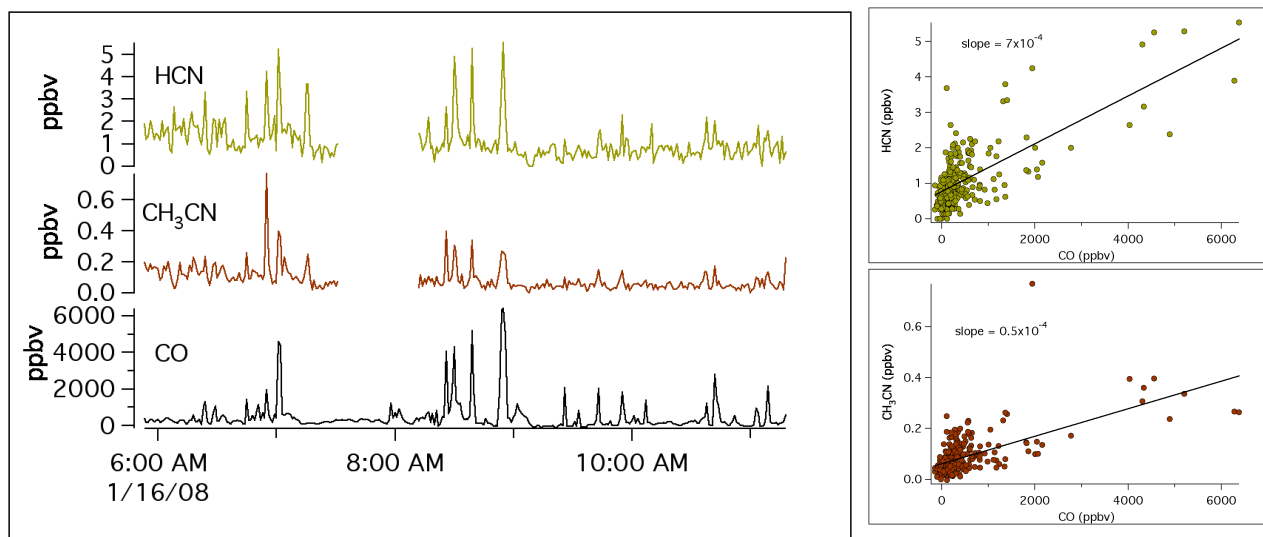


Figure 4-10. On-road measurements of vehicle exhaust emissions of HCN and  $\text{CH}_3\text{CN}$  in the Boston metro area.

#### 4.4 Carbonaceous aerosol processing in the Mexico City metropolitan Area

The Mexico City Metropolitan Area is a mega-city environment with significant air pollution. Emissions of primary particles and secondary particle precursors are high and build up in the boundary layer during the night with the concentrations peaking during the early morning. Daily photochemistry alters the chemical, physical, and optical properties of these primary particles. The Aerodyne mobile laboratory, outfitted with a suite of gas and particle instruments, investigated the processing of these primary particles at the T0 site as part of the Mexico City Metropolitan Area (MCMA) component of the MILAGRO campaign (March 2006). Figure 4-11 shows the mobile laboratory during sampling.

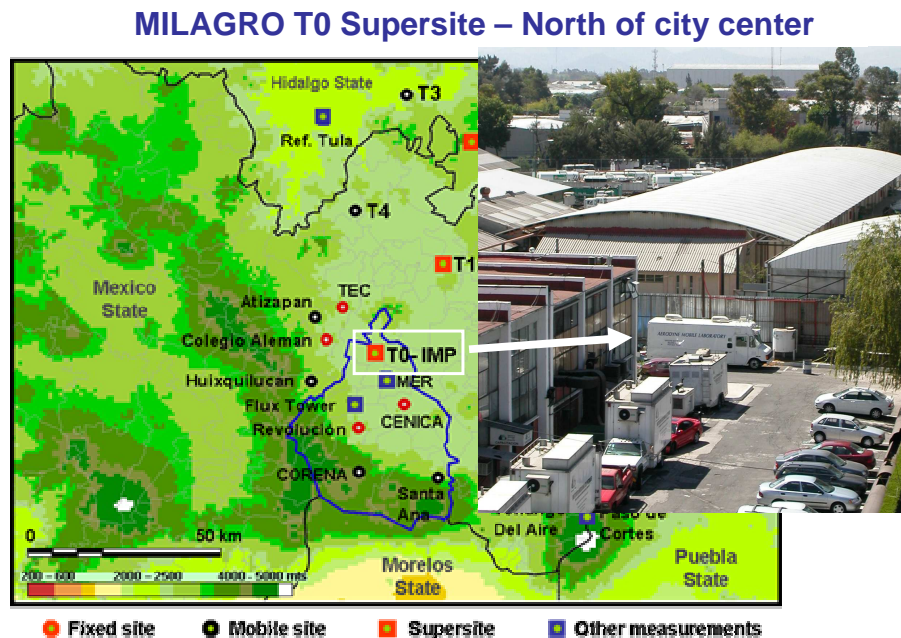


Figure 4-11. Aerodyne mobile laboratory sampling at T0 supersite.

Aerosol particle mass, chemistry (bulk and surface PAHs), absorption and scattering, and size-distributions (mobility and vacuum aerodynamic) were measured. Diurnal traces shown in Figure 4-12 from T0 show the strong correlation between black carbon particle mass, total reactive nitrogen oxides ( $\text{NO}_y$ ), and carbon dioxide suggesting strong vehicular emissions during early morning rush hour. Emissions concentrations decrease significantly after the sun has risen as the boundary layer rises and dilutes the emissions. Interestingly, carbon monoxide does not appear to be as well correlated with the other primary combustion emission markers and appears to lag behind them during the very early morning hours.

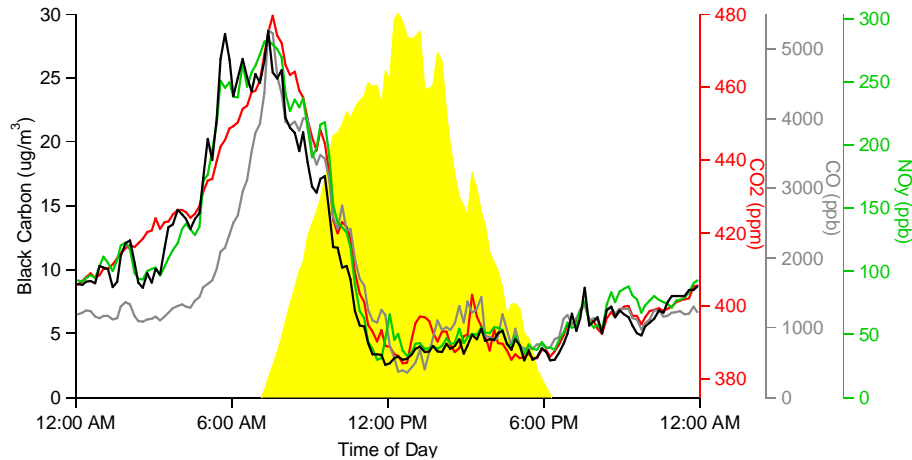


Figure 4-12. Diurnal concentrations of black carbon, NO<sub>y</sub>, carbon dioxide, and carbon monoxide at T0.

Figure 4-13 shows the diurnally averaged correlation between the black carbon PM and carbon monoxide. The resulting correlation indicates two different emission sources for both BC and CO. The morning source has a higher BC/CO ratio (0.019 ug/m<sup>3</sup>/ppb) than the mid-day source (0.0048 ug/m<sup>3</sup>/ppb). A potential explanation is that the early morning traffic in Mexico City is more influenced by diesel truck traffic than later in the day as businesses bring materials (e.g. food, etc.) into the city in preparation for daily life.

The Aerodyne Aerosol Mass Spectrometer (AMS) measured the non-refractory PM<sub>1.0</sub> aerosol mass loading and particle vacuum aerodynamic diameter. Using known and laboratory tested fragmentation patterns and Positive Matrix Factorization (PMF) methods, the average aerosol mass spectra were deconvolved to provide mass loadings for various inorganic and organic species. The PM at T0 was dominated throughout most of the day by Hydrocarbon-like Organic Aerosol (HOA) mass, though Oxidized Organic Aerosol (OOA) was observed to dominate during afternoon hours. The PM HOA is well correlated with the black carbon PM, carbon dioxide, NO<sub>y</sub>, and carbon monoxide,

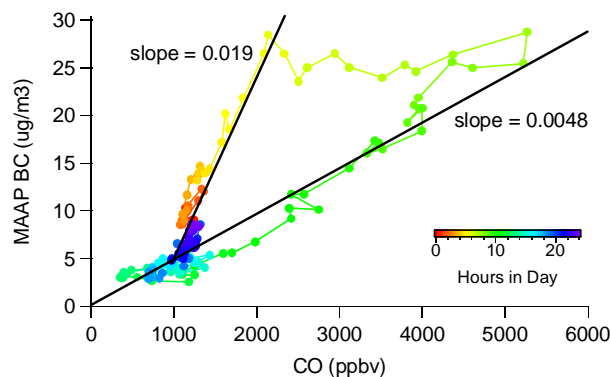


Figure 4-13. Diurnally averaged correlation between black carbon PM and gas phase CO at T0.

suggesting that most of the HOA is likely traffic and industry related Primary Organic Aerosol (POA). The OOA correlates well with photochemical markers and is likely formed through Secondary Organic Aerosol (SOA) processes. Figure 4-14 shows the diurnal averages for the organic aerosol components at T0.

Biomass burning has been identified as a potentially significant source for carbonaceous (organic and elemental carbon) aerosol in the Mexico City Metropolitan Area (MCMA). Results from our preliminary PMF analysis do indicate that Biomass Burning Organic Aerosol (BBOA) markers exist in the data; however, the markers suggest that near the city center (T0), the BBOA is a minor fine PM component. The BBOA markers peak in the mid-morning with carbon monoxide, acetonitrile, and particulate chloride. The presence of particulate chloride associated with BBOA markers may indicate that some of the burning may be due to refuse burning throughout the city during the morning hours.

One of our focuses during MCMA 2006 study was to investigate the emissions and transformations of carbonaceous soot particles during the early morning hours. The goal was to understand what happens to these particles (which obviously dominate the PM loadings during morning hours) after they are emitted. Towards these goals, we set up a soot particle experiment at T0 during the last three days of the MCMA 2006 study. The study consisted of measuring mobility size selected particles with an SMPS, AMS, and black carbon instruments to investigate the changes in the carbonaceous soot particles morphologies and chemical compositions (e.g. coatings). A schematic of the study instrumental setup is shown in Figure 4-15.

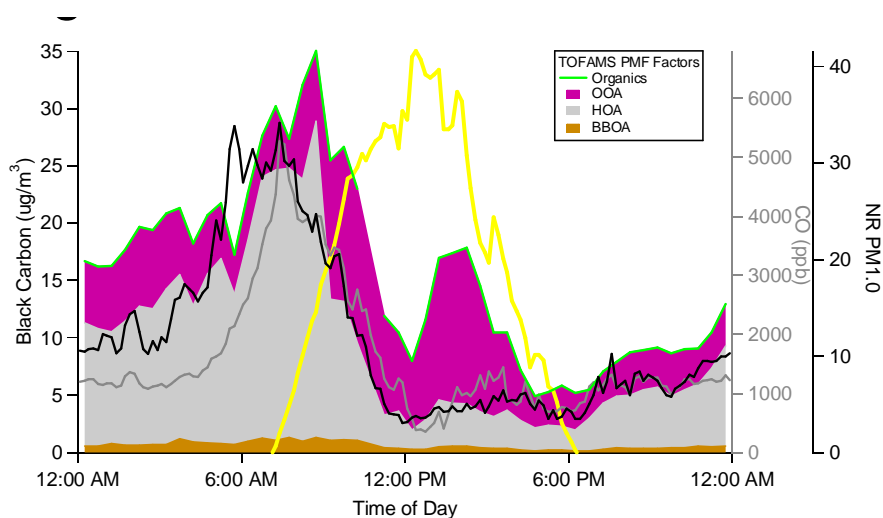


Figure 4-14. Diurnal PM loadings for Organic Aerosol PMF factors at T0.



## Schematic for studying carbonaceous particle production and processing

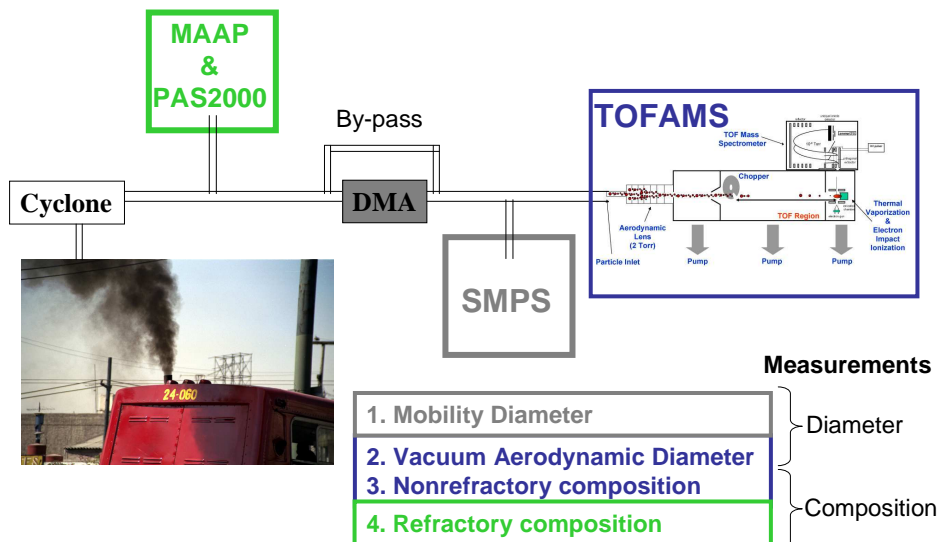


Figure 4-15. Soot particle experimental setup.

The experimental method consisted of switching between sampling ambient air and sampling size selected particles behind a Differential Mobility Analyzer (DMA). Figure 4-16 shows AMS results as we switched between sampling ambient air and the low, but real, aerosol mass signal after selecting single particle sizes through a DMA.

Size selected particles that passed through the DMA exhibited two distinctly different particle effective densities. Particles with different effective densities are well separated in the AMS due to their subsequently different vacuum aerodynamic diameters ( $D_{va}$ ;  $D_{va}$

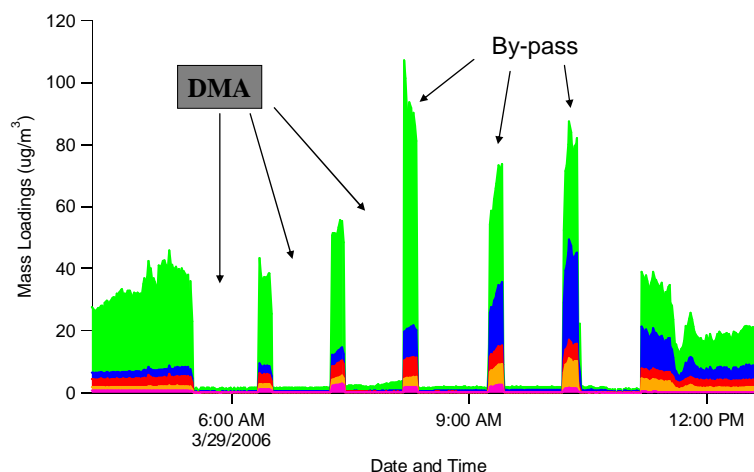


Figure 4-16. Experimental method.

$\sim \rho_{\text{effective}} * D_{\text{mobility}}$ ). Figure 4-17 shows an average ensemble size distribution for the AMS and SMPS for ambient sampling (top plot) and the size-selected ( $D_{va} = 215$  nm) results in the bottom plot. The bottom plot shows the two distinct aerosol modes. Fractal-like carbonaceous soot particles exhibit a lower effective density than more spherical accumulation mode particles. Thus, the lower  $D_{va}$  particles are the fractal-like carbonaceous soot particles that have been freshly emitted from the traffic (and other combustion sources) in the near vicinity of T0.

By monitoring the two size-selected particle modes in time during the morning transition from a low boundary layer to a high daily mixing layer after sun rise and into late morning/early afternoon, we have been able to track the rapid transformation of the freshly emitted fractal-like carbonaceous soot particles into more condensed accumulation mode particles. Figure 4-18 shows this transformation as the smaller  $D_{va}$  organic particle mode increases in vacuum aerodynamic diameter (decreases in effective density) during the morning hours.

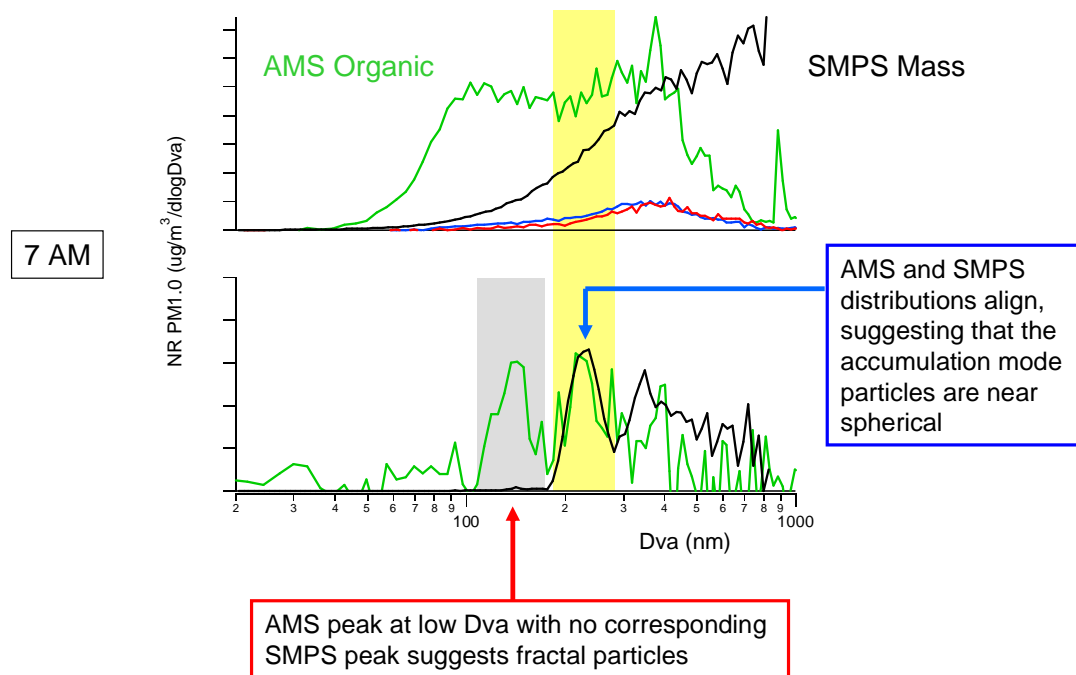


Figure 4-17. Ambient polydisperse and size-selected monodisperse aerosol sampled by the AMS and SMPS.

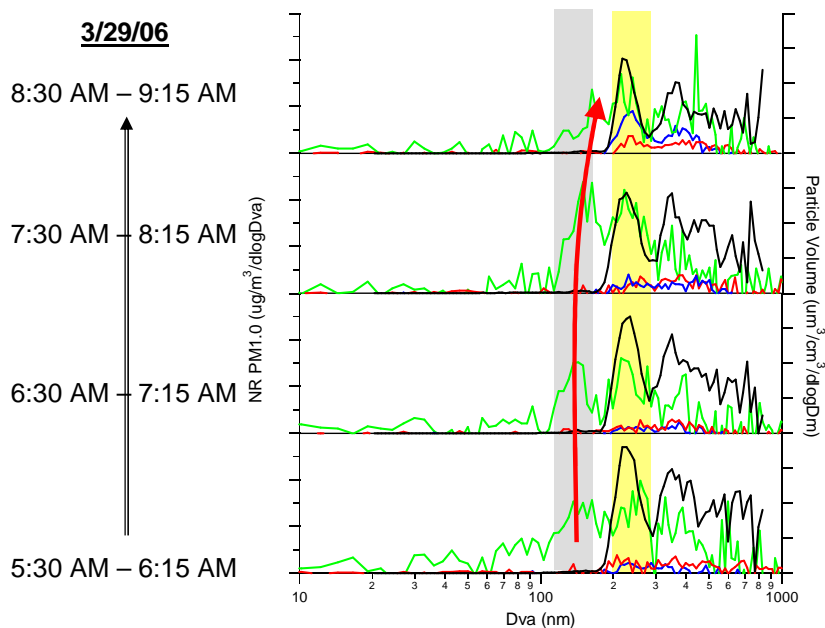


Figure 4-18. Time evolution of fractal-like carbonaceous soot particles as a function of time during morning hours at T0.

Following the analysis methods outlined in (Slowik et al., 2004)., simultaneous measurements by the AMS and SMPS instruments on mobility-selected particles yielded carbonaceous soot particle mass, volume, density, composition, dynamic shape factor, and fractal dimension. Figure 4-19 shows the evolution of the fractal-like carbonaceous soot particle mass and shape as a function of time-of-day. As the morning progressed, particles become larger (greater mass) and more spherical. These transformations are likely due to condensational growth from photochemical reactions (i.e. secondary aerosol products).

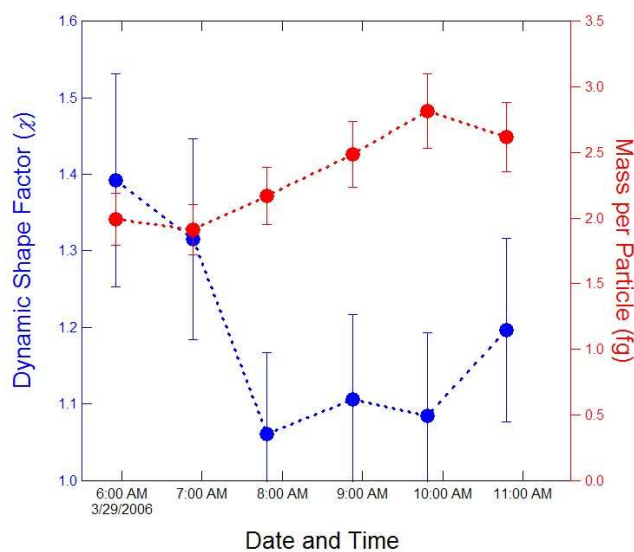


Figure 4-19. Evolution of fractal-like carbonaceous soot particle mass and shape at T0.

Another measure of carbonaceous soot particle surface chemistry measured during the T0 soot experiment was the combination of the MAAP black carbon PM measurements and the surface Polycyclic Aromatic Hydrocarbon (PAH) concentrations measured by the Ecochem Photoelectric Aerosol Sensor (PAS). The ratio of the surface PAH concentration of the BC PM loading provides a measure of the “fresh” carbonaceous surface of the emitted soot particles. Figure 4-20 shows the size-selected particle results compared with the surface PAH/BC PM ratio as a function of time-of-day.

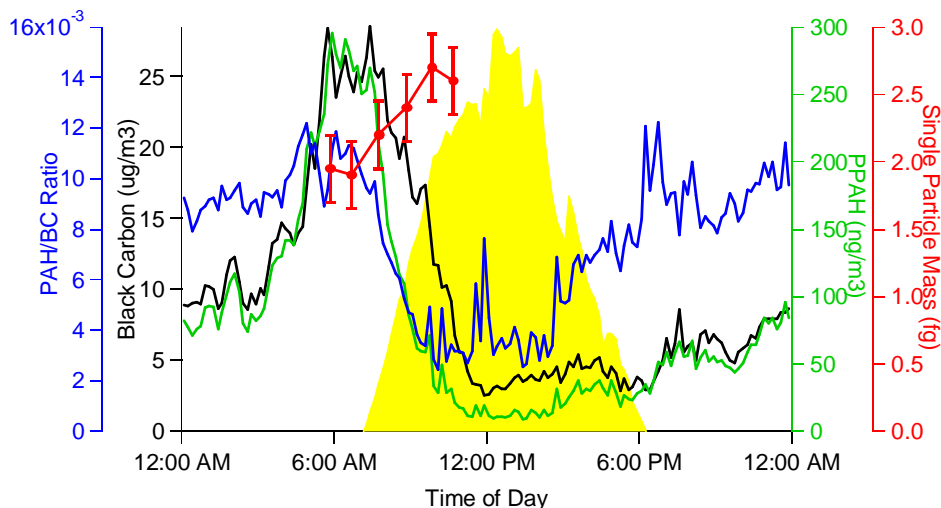


Figure 4-20. Comparison of the surface-bound PAH/BC ratio and the size-selected soot particle results.

It is readily apparent from Figure 4-20 that the fractal-like carbonaceous soot particles emitted in large quantities during the morning hours in Mexico City both gain particle mass, become more spherical, and lose their surface PAH concentrations at the same time that the sun starts to rise. Primary soot particles are rapidly coated with photo-oxidation products, changing their surface chemistry and shape.

Due to the rapid condensational processes that begin nearly simultaneously with the rise of the sun, it is likely that the emitted carbonaceous soot particles become rapidly coated and established as elemental carbon cores in the accumulation mode particles that get transported downwind and out of the MCMA basin. A remaining challenge is to understand what happens to these coated carbonaceous particle cores. Do they represent the HOA measured at other locations within MCMA? Despite the rapid coating, are they also subjugated to rapid photochemical oxidation reactions that convert their carbonaceous carbon into OOA and volatile gas phase species? Figure 4-21 shows the average OOA, HOA, and PPAH/BC values measured at several different locations within MCMA. The HOA/OOA and PPAH/BC ratios both decrease with distance from the major carbonaceous particle sources (e.g. traffic) at the city center.

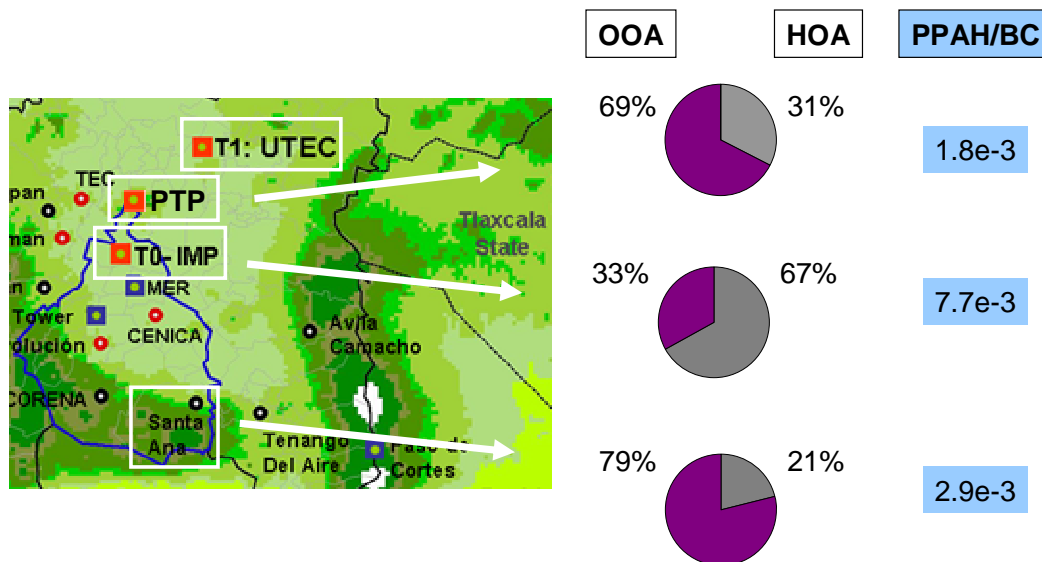


Figure 4-21. Average OOA and HOA PM fractions and PPAH/BC ratios measured at various locations within MCMA during the MCMA2006 study.

Results from our T0 soot experiment indicate that in the Mexico City urban environment, carbonaceous soot particles appear to be dominated by traffic composition (heavy duty diesel and lighter duty gasoline vehicles) with little biomass burning influence. Early morning primary particle emissions were dominated by fractal particles containing significant surface bound PAH's, similar in morphology and composition to diesel-generated particles. During the morning, these particles were observed to grow in mass and become more spherical via gas-to-particle condensation of photochemical products (oxidized organic compounds and ammonium nitrate). Particles with fractal morphologies and surface bound PAH signals were no longer evident after late morning and at down wind locations. The transportation of particles from sources near the city center to boundary sites correlates with more oxidized organic compounds and lower PAH/BC ratios.

The following manuscript is in preparation:

**Onasch, T. B. et al., Carbonaceous aerosol processing in Mexico City.**

#### 4.5 Determination of urban plume photochemical age

The relative isolation of the PTP site from local emission sources make it an ideal location for studying changes as the MCMA urban plume aging. Insights gained are not limited to particulate matter as discussed in section 4.1. The plume's gas phase composition reveals active photo-oxidation in the early urban plume mixing and dilution

stages. Figure 4.22 depicts the diurnal profile for several aromatic and oxygenated VOCs measured with the PTR-MS. The dominant daylight photochemical sink for most VOC species is reaction with the hydroxyl radical. The rate constant for the reaction of OH with benzene is  $\sim 1 \times 10^{-12}$  molecules<sup>-1</sup> cm<sup>3</sup> s<sup>-1</sup> while the effective rate constant for the reaction of OH radical with the C3-benzene compounds is 17 times greater. This difference in rate constants provides a useful clock to estimate the photochemical age of the airmass. In the right-top panel the correlation of C3-benzene to benzene shows the darker (nighttime) points are close to the actual emission ratio, as measured at the T0 site. The data points with increasing yellow represent the daylight values showing that the c3-benzene compounds have been reactively depleted relative to benzene. Acetone and acetaldehyde (right-middle and right-bottom panels) show the opposite behavior since they are produced by photochemical activity.

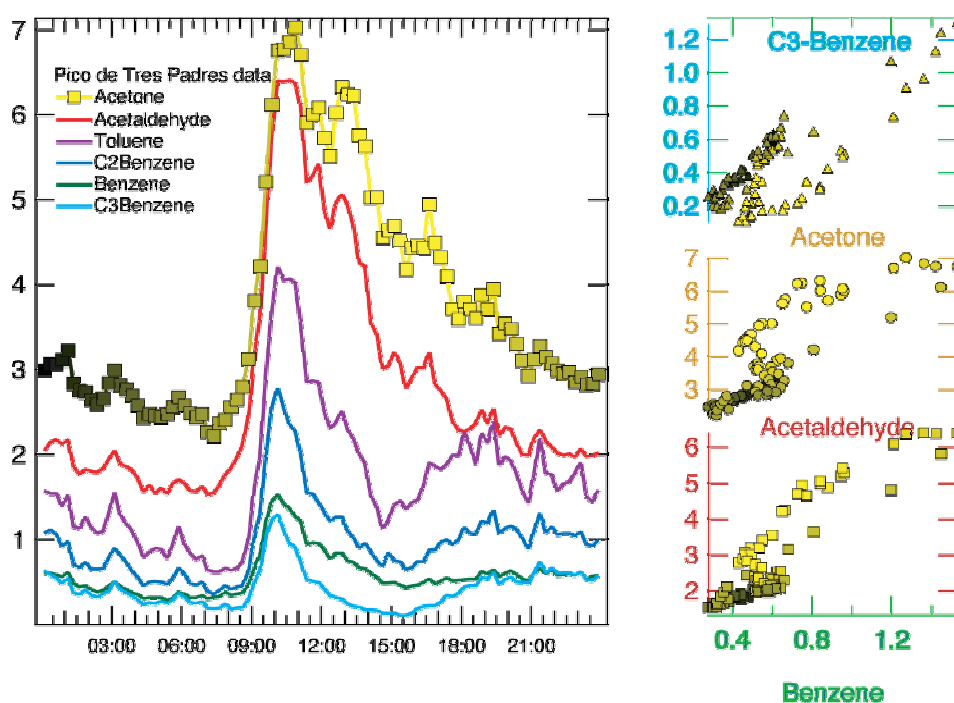


Figure 4-22. Diurnal aromatic and oxygenated VOC profile at PTP. The panel on the left depicts the mixing ratios (ppbv) of selected VOCs. The panel on the right shows, from top to bottom, the C3-benzene, acetone and acetaldehyde correlation plots with benzene colored by time of day (darker points - night, lighter points - day).

Analyses of these VOC measurements allow a deeper understanding of both the gas phase and particle secondary pollutant production processes by providing a photochemical (kinetic) clock that can be used to characterize and correlate the production of photochemical intermediates and secondary products. These analyses are critical input for the SOA production and gas phase photo-oxidation intermediate and product analyses discussed in sections 4.1 and 4.2.

## 5. Summary

This project supported the participation of ARI and MSU scientists in the MCMA-2006 project along with collaborating research personnel from the MIT/MCE2 and UC groups led by L.T. Molina and J.L Jimenez. MCMA-2006 focused on: 1) the primary emissions of fine particles and precursor gases leading to photochemical production of atmospheric oxidants and secondary aerosol particles and 2) the measurement and analysis of secondary oxidants and secondary fine particular matter (PM) production, with particular emphasis on secondary organic aerosol (SOA). This work supported the MAX-Mex/MILAGRO field campaign that investigated the near field and long range evolution and impacts of the Mexico City urban plume in March 2006.

MCMA-2006 pursued its goals through three main activities: 1) performance and publication of detailed analyses of extensive MCMA trace gas and fine PM measurements made by the collaborating groups and others during earlier MCMA field campaigns in 2002 and 2003; 2) deployment and utilization of extensive real-time trace gas and fine PM instrumentation at urban and downwind MCMA sites in support of the MAX-Mex/MILAGRO field measurements in March, 2006; and, 3) analyses of the 2006 MCMA data sets leading to further publications drawing on the new data as well as insights from analysis and publication of the 2002/2003 field data.

With partial support from this project ARI and MSU scientists, in collaboration with a range of U.S. colleagues (including MIT/MCE2 and CU) and Mexican collaborators, completed analysis of several extensive data sets from the earlier MCMA-2002/2003 campaigns and co-authored thirteen archival papers published in 2005-2007. The substance and impact of these papers was discussed in Section 2 of this report and they are listed in Section 6.1.

The Aerodyne mobile laboratory, outfitted with real-time trace gas and fine PM instrumentation from five collaborating laboratories (including ARI and MSU) was deployed to a wide range of carefully selected MCMA urban, industrial, downwind and background sites during March 2006, spanning the MILAGRO campaign time frame. In addition, it measured on-road fleet average vehicle emissions while in transit between measurement sites, generating valuable vehicle emissions inventory data to update those gathered during MCMA-2002/2003. An overview of the deployment sites and some analysis results from the on-road vehicle emissions measurements were presented in Section 3.

Analyses of four components of the MCMA-2006 fixed site data, organic aerosol composition and secondary formation rate, links between nitrogen oxide speciation, free radical production and ozone formation, urban sources of cyanide tracer species, and the aging of primary carbonaceous aerosol particles, were presented in Section 4. A list of MCMA-2006 data analyses manuscripts already submitted for publication is presented in Section 6.2 and additional manuscripts in preparation are identified in the text of Sections 3 and 4.

Analysis results and publications from the MCMA-2002/2003 and MCMA-2006 measurements have been conveyed to Mexican government and academic scientists who are using them to devise and evaluate air quality management strategies for the MCMA. In addition, they have been widely shared with MAX-Mex and other MILAGRO research groups to aid in their data analysis and model development tasks focused on evaluating regional and continental scale climate impacts of megacity emissions.

Finally, collaborations have been formed with modeling groups at MCE2, PNNL, Georgia Tech, and CMU that are expected to result in further publishable analyses and data/simulation comparisons.



## 6. Project Publications and Other Technical References

### 6.1 Project Publications Based on MCMA-2002/2003 Data Analyses

1. Jiang, M., Marr, L. C., Dunlea, E. J., Herndon, S. C., Jayne, J. T., Kolb, C. E., Knighton, W. B., Rogers, T. M., Zavala, M., Molina, L. T., Molina, M. J., **Vehicle Fleet Emissions of Black Carbon, Polycyclic Aromatic Hydrocarbons, and Other Pollutants Measured by a Mobile Laboratory in Mexico City**, *Atmos. Chem. Phys.*, 5, 3377-3387, 2005.
2. Salcedo, D., Onasch, T. B., Dzepina, K., Canagaratna, M. R., Zhang, Q., Huffman, J. A., DeCarlo, P. F., Jayne, J. T., Mortimer, P., Worsnop, D. R., Kolb, C. E., Johnson, K. S., Zuberi, B., Marr, L. C., Volkamer, R., Molina, L. T., Molina, M. J., Cardenas, B., Bernabe, R. M., Marquez, C., Gaffney, J. S., Marley, N. A., Laskin, A., Shutthanandan, V., Xie, Y., Brune, W., Leshner, R., Shirley, T., Jimenez, J. L., **Characterization of Ambient Aerosols in Mexico City during the MCMA-2003 Campaign with Aerosol Mass Spectrometry: results from the CENICA Supersite**, *Atmos. Chem. Phys.*, 6, 925-946, 2006.
3. Dunlea, E. J., Herndon, S. C., Nelson, D. D., Volkamer, R. M., Lamb, B. K., Allwine, E. J., Grutter, M., Ramos Villegas, C. R., Marquez, C., Blanco, S., Cardenas, B., Kolb, C. E., Molina, L. T., Molina, M. J., **Technical note: Evaluation of Standard Ultraviolet Absorption Ozone Monitors in a Polluted Urban Environment**, *Atmos. Chem. Phys.*, 6, 3163-3180, 2006.
4. Garcia, A. R., Volkamer, R., Molina, L. T., Molina, M. J., Samuelson, J., Mellqvist, J., Galle, B., Herndon, S. C., Kolb, C. E., **Separation of Emitted and Photochemical Formaldehyde in Mexico City Using a Statistical Analysis and a New Pair of Gas-Phase Tracers**, *Atmos. Chem. Phys.*, 6, 4545-4557, 2006.
5. San Martini, F. M., Dunlea, E. J., Grutter, M., Onasch, T. B., Jayne, J. T., Canagaratna, M. R., Worsnop, D. R., Kolb, C. E., Shorter, J. H., Herndon, S. C., Zahniser, M. S., Ortega, J. M., McRae, G. J., Molina, L. T., Molina, M. J., **Implementation of a Markov Chain Monte Carlo Method to Inorganic Aerosol Modeling of Observations from the MCMA-2003 Campaign. Part I: Model Description and Application to the La Merced Site**, *Atmos. Chem. Phys.*, 6, 4867-4888, 2006.

6. San Martini, F. M., Dunlea, E. J., Volkamer, R., Onasch, T. B., Jayne, J. T., Canagaratna, M. R., Worsnop, D. R., Kolb, C. E., Shorter, J. H., Herndon, S. C., Zahniser, M. S., Salcedo, D., Dzepina, K., Jimenez, J. L., Ortega, J. M., Johnson, K. S., McRae, G. J., Molina, L. T., Molina, M. J., **Implementation of a Markov Chain Monte Carlo Method to Inorganic Aerosol Modeling of Observations from the MCMA-2003 Campaign. Part II: Model Application to the CENICA, Pedregal and Santa Ana Sites**, *Atmos. Chem. Phys.*, 6, 4889-4904, 2006.
7. Zavala, M., Herndon, S. C., Slott, R. S., Dunlea, E. J., Marr, L. C., Shorter, J. H., Zahniser, M., Knighton, W. B., Rogers, T. M., Kolb, C. E., Molina, L. T., Molina, M. J., **Characterization of On-Road Vehicle Emissions in the Mexico City Metropolitan Area Using a Mobile Laboratory in Chase and Fleet Average Measurement Modes during the MCMA-2003 Field Campaign**, *Atmos. Chem. Phys.*, 6, 5129-5142, 2006.
8. Volkamer, R., Jimenez, J. L., San Martini, F., Dzepina, K., Zhang, Q., Salcedo, D., Molina, L. T., Worsnop, D. R., Molina, M. J., **Secondary Organic Aerosol Formation from Anthropogenic Air Pollution: Rapid and Higher than Expected**, *Geophys. Res. Lett.* doi: 10. 1029/2006GL026899, 2006.
9. Velasco, E., Lamb, B., Westberg, H., Allwine, E., Sosa, G., Arriaga-Colina, J. L., Jobson, B. T., Alexander, M. L., Prazeller, P., Knighton, W. B., Rogers, T. M., Grutter, M., Herndon, S. C., Kolb, C. E., Zavala, M., de Foy, B., Volkamer, R., Molina, L. T., Molina, M. J., **Distribution, Magnitudes, Reactivities, Ratios and Diurnal Patterns of Volatile Organic Compounds in the Valley of Mexico during the MCMA 2002 and 2003 Field Campaigns**, *Atmos. Chem. Phys.*, 7, 329-353, 2007.
10. Salcedo, D., Onasch, T. B., Canagaratna, M. R., Dzepina, K., Huffman, J. A., Jayne, J. T., Worsnop, D. R., Kolb, C. E., Weimer, S., Drewnick, F., Allan, J. D., Delia, A. E., Jimenez, J. L., **Technical Note: Use of a Beam Width Probe in an Aerosol Mass Spectrometer to Monitor Particle Collection Efficiency in the Field**, *Atmos. Chem. Phys.*, 7, 549-556, 2007.
11. Dunlea E. J., Herndon, S. C., Nelson, D. D., Volkamer, R. M., San Martini, F., Sheehy, P. M., Zahniser, M. S., Shorter, J. H., Wormhoudt, J. C., Lamb, B. K., Allwine, E. J., Gaffney, J. S., Marley, N. A., Grutter, M., Marquez, C., Blanco, S., Cardenas, B., Retama, A., Ramos Villegas, C. R., Kolb, C. E., Molina, L. T., Molina, M. J., **Evaluation of Nitrogen Dioxide Chemiluminescence Monitors in a Polluted Urban Environment**, *Atmos. Chem. Phys.*, 7, 2691-2704, 2007.

12. Dzepina, K., Arey, J., Marr, L. C., Worsnop, D. R., Salcedo, D., Zhang, Q., Onasch, T. B., Molina, L. T., Molina, M. J., Jimenez, J. L., **Detection of Particle-Phase Polycyclic Aromatic Hydrocarbons in Mexico City Using an Aerosol Mass Spectrometer**, *Int. J. Mass Spectrometry*, 263(2-3), 152-170, 2007.
13. Molina, L. T., Kolb, C. E., de Foy, B., Lamb, B. K., Brune, W. H., Jimenez, J. L., Ramos-Villegas, R., Sarmiento, J., Paramo-Figueroa, V. H., Cardenas, B., Gutierrez-Avedoy, V., Molina, M. J., **Air quality in North America's most populous city – overview of MCMA-2003 Campaign**, *Atmos. Chem. Phys.*, 7, 2447-2473, 2007.

## 6.2 Manuscripts Submitted for Publication

1. Thornhill, D. A., Herndon, S. C., Onasch, T. B., Wood, E. C., Zavala, M., Molina, L. T., Gaffney, J. S., Marley, N. A., and Marr, L. C.: **Particulate polycyclic aromatic hydrocarbon spatial variability and aging in Mexico City**, *Atmos. Chem. Phys. Discuss*, 7, 15693-15721, 2007.
2. S.C. Herndon, T.B. Onasch, E.C. Wood, J.H. Kroll, M.R. Cengaratna, J. T. Jayne, M.A. Zavala, W.B. Knighton, C. Mazzoleni, M.K. Dubey, I.M. Ulbrich, J.L. Jimenez, R. Seila, J.A. de Gouw, B. de Foy, J. Fast, L.T. Molina, C.E. Kolb and D.R. Worsnop, **The correlation of secondary organic aerosol with odd oxygen in a meagacity outflow**, *Geophys. Res. Lett.*, submitted, 2008.

## 6.3 Technical References

Baum, M. M., J. A. Moss, Pastel, S. H., Poskrebyshev, G. A., (2007). Hydrogen cyanide exhaust emissions from in-use motor vehicles. *Environ. Sci. & Technol.* 41, 857-862.

CAM (Comisión Ambiental Metropolitana): Inventario de Emisiones 2004 de la Zona Metropolitana del Valle de México, México, 2006.

de Gouw, J. A., Middlebrook, A.M., Warneke, C., Goldan, P.D., Kuster, W.C., Roberts, J. M., Fehsenfeld, F. C., Worsnop, D. R., Cengaratna, M.R., Pszenny, A. A. P., Keene, W. C., Marchewka, M., Bertman, S. B., Bates, T. S., (2005), Budget of organic carbon in a polluted atmosphere: Results from the New England Air Quality Study in 2002, *J. Geophys. Res. Atmos.* 110, doi: 10.1029/2004JD005623.

Farmer, D. (2008), Personal Communication

Flocke, F. (2008), Personal Communication

Heald, C. L., Jacob, D.J., Park, R.J., Russell, L.M., Huebert, B.J., Seinfeld, J.H., Liao, H., Weber, R.J. (2005), A large organic aerosol source in the free troposphere missing from current models, *Geophys. Res. Lett.*, 32, doi:10.1029/2005GL023831.

Karlsson, H. L. (2004). Ammonia, nitrous oxide and hydrogen cyanide emissions from five passenger vehicles. *Sci. Total Environ.* 334-335: 125-132.

Kleinman, L. I. (2005), The dependence of tropospheric ozone production rate on ozone precursors, *Atmos. Environ.*, 39, 575-586.

Kleinman, L. I., P. H. Daum, Y. N. Lee, L. J. Nunnermacker, S. R. Springston, J. Weinstein-Lloyd, and J. Rudolph (2005), A comparative study of ozone production in five U.S. metropolitan areas, *J. Geophys. Res. Atmos.*, 110, doi:10.1029/2005JD005760.

Kleinman, L. I., Springston, S. R., Daum, P. H., Lee, Y. -N., Nunnermacker, L. J., Senum, G. I., Wang, J., Weinstein-Lloyd, J., Alexander, M. L., Hubbe, J., Ortega, J., Canagaratna, M., Jayne, J., (2008). The time evolution of aerosol composition over the Mexico City plateau. *Atmos. Chem. Phys.* 8, 1559-1575.

Kolb, C. E., Herndon, S. C., McManus, B., Shorter, J. H., Zahniser, M. S., Nelson, D. D., Jayne, J. T., Canagaratna, M. R., Worsnop, D. R., (2004), Mobile Laboratory with Rapid Response Instruments for Real-Time Measurements of Urban and Regional Trace Gas and Particulate Distributions and Emission Source Characteristics, *Environ. Sci. Technol.*, 38, 5694-5703.

Lanz, V.A., Alfarra, M. R., Baltensperger, U., Buchmann, B., Hueglin, C., Prevot, A.S.H., (2007), Source apportionment of submicron organic aerosols at an urban site by factor analytical modeling of aerosol mass spectra, *Atmos. Chem. Phys.* 7, 1503-1522.

Lei, W., B. de Foy, M. Zavala, R. Volkamer, and L. T. Molina (2007), Characterizing ozone production in the Mexico City Metropolitan Area: a case study using a chemical transport model, *Atmos. Chem. Phys.*, 7, 1347-1366.

Rogers, T. M., Grimsrud, E.P., Herndon, S.C., Jayne, J.T., Kolb, C.E., Allwine, E., Westberg, H., Lamb, B.K., Zavala, M., Molina, L.T., Molina, M.J., Knighton, W.B., (2006). On-road measurements of volatile organic compounds in the Mexico City metropolitan area using proton transfer reaction mass spectrometry. *Int. J. Mass Spectrom.* 252, 26-37.

Shim, C. S., Y. H. Wang, Singh, H. B., Blake, D. R., Guenther, A. B. (2007). Source characteristics of oxygenated volatile organic compounds and hydrogen cyanide. *J. Geophys. Res. Atmos.* 112, doi:10.1029/2006JD007543.

Slowik, J.G. et al., (2004) Particle morphology and density characterization by combined mobility and aerodynamic diameter measurements. Part 2: Application to combustion generated soot aerosols as a function of fuel equivalence ratios, *Aerosol Sci. Technol.* 38: 1206-1222.

Spaniel, P., Wang, T., Smith, D., (2004). Quantification of hydrogen cyanide in humid air by selected ion flow tube mass spectrometry. *Rapid Communications in Mass Spectrometry* 18, 1869-1873.

Volkamer, R., Jimenez, J.L., SanMartini, F., Dzepina, K., Zhang, Q., Salcedo, D., Molina, L.T., Worsnop, D.R., Molina, M.J., (2006), Secondary organic aerosol formation from anthropogenic air pollution: Rapid and higher than expected, *Geophys. Res. Lett.* 33, doi: 10.1029/2006GL02689.

Yokelson, R. J., Urbanski, S. P., Atlas, E. L., Toohey, D. W., Alvarado, E. C., Crounse, J. D., Wennberg, P. O., Fisher, M. E., Wold, C. E., Campos, T. L., Adachi, K., Buseck, P. R., Hao, W. M., (2007). Emissions from forest fires near Mexico City. *Atmos. Chem. Phys.* 7 5569-5584.

Zavala, M., Herndon, S. C., Slott, R. S., Dunlea, E. J., Marr, L. C., Shorter, J. H., Zahniser, M., Knighton, W. B., Rogers, T. M., Kolb, C. E., Molina, L. T., & Molina, M. (2006) Characterization of on-road vehicle emissions in the Mexico City Metropolitan Area using a mobile laboratory in chase and fleet average measurement modes during the MCMA-2003 field campaign. *Atmos. Chem. Phys.*, 6, 5129–5142.

Zhang, Q., Worsnop, D. R., Canagaratna, M. R., Jimenez, J. L., (2005), Hydrocarbon-like and oxygenated organic aerosols in Pittsburgh: insights into sources and processes of organic aerosols, *Atmos. Chem. Phys.* 5, 3289-3311.

Zhang, Q., Jimenez, J. L., Canagaratna, M. R., Allan, J. D., Coe, H., Ulbrich, I., Alfarra, M. R., Takami, A., Middlebrook, A. M., Sun, Y. L. Dzepina, K., Dunlea, E., Docherty, K., DeCarlo, P. F., Salcedo, D., Onasch, T., Jayne, J. T., Miyoshi, T., Shimojo, A., Hatakeyama, S., Takegawa, N., Kondo, Y., Schneider, J., Drewnick, F., Borrmann, S., Weimer, S., Demerjian, K., Williams, P., Bower, K., Bahreini, R., Cottrell, L., Griffin, R. J., Rautiainen, J., Sun, J. Y., Zhang, Y. M., Worsnop, D. R., (2007), Ubiquity and dominance of oxygenated species in organic aerosols in anthropogenically-influenced Northern Hemisphere midlatitudes, *Geophys. Res. Lett.* 34, doi: 10.1079/GL029979.